Lethaia
AN INTERNATIONAL JOURNAL OF PALAEONTOLOGY AND STRATIGRAPHY

A proposed new global stratotype for Aeronian Stage of the Silurian System: Hlásná Třebaň section, Czech Republic

PETR ŠTORCH, ŠTĚPÁN MANDA, ZUZANA TASÁRYOVÁ, JIŘÍ FRÝDA, LEONA CHADIMOVÁ AND MICHAEL J. MELCHIN

LETHAIA

Štorch, P., Manda, Š., Tasáryová, Z., Frýda, J., Chadimová, L. & Melchin, M.J. 2018: A proposed new global stratotype for Aeronian Stage of the Silurian System: Hlásná Třebaň section, Czech Republic. *Lethaia*, Vol. 51, pp. 357–388.

The current Global Stratotype Section and Point (GSSP) for the Aeronian Stage (Llandovery Series, Silurian System), on Trefawr track in the Llandovery area of Wales, is an inadequate marker for precise, global, correlation. The International Subcommission on Silurian Stratigraphy has, therefore, undertaken the selection of a new GSSP for this level. The lowest occurrence of the graptolite *Demirastrites triangulatus*, 1.38 m above the base of the black-shale succession of the Želkovice Formation at the Hlásná Třebaň section in Central Bohemia, is proposed to mark the base of the Aeronian Stage. The section, which fulfils all formal requirements for stratotype of a chronostratigraphical unit, should be considered as a candidate for the new GSSP. An abundant, well-preserved, diverse graptolite fauna occurs through the section along with common chitinozoans, which indicate that the *Spinachitina maennili* Biozone spans the boundary interval. The section comprises the lower–middle Aeronian (*D. triangulatus*–*Lituigraptus convolutus* graptolite biozones) along with underlying Rhuddanian (*Akidograptus ascensus*–*Coronograptus cyphus* biozones) and Hirnantian strata. Several graptolite genera of primary importance in global correlation (*Demirastrites*, *Petalolithus*, *Rastrites* and *Campograptus*) first appear in the lower part of the *triangulatus* Biozone. The structurally simple section is somewhat condensed, but there is a uniform succession of black shale without any evidence of disconformity in the broad boundary interval. The C_{org} isotope record exhibits a minor positive excursion just above the base of the *triangulatus* Biozone, whereas TOC and N isotope and elemental geochemical records provide evidence for uninterrupted sedimentation under stable, anoxic conditions. ☐ *Aeronian, geochemistry, graptolites, GSSP proposal, Silurian.*

Petr Štorch ✉ [storch@gli.cas.cz], and Leona Chadimová [chadimova@gli.cas.cz], Institute of Geology CAS, Rozvojová 269, 165 00 Praha 6, Czech Republic; Štěpán Manda [stepan.manda@geology.cz], Zuzana Tasáryová [zuzana.tasaryova@geology.cz], and Jiří Frýda [bellerophon@seznam.cz], Czech Geological Survey, Klárov 3 118 21, Praha 1, Czech Republic; Michael J. Melchin [mmelchin@stfx.ca], St. Francis Xavier University, Antigonish, NS B2G 2W5, Canada; *manuscript received on 25/02/2017; manuscript accepted on 24/08/2017.*

The Silurian System was the first Phanerozoic System in which all boundary stratotypes of the respective series and stages were formally established. With a single exception, all Silurian stratotypes defined in the 1980s (Holland & Bassett 1989) were selected in classic Palaeozoic terrains of Great Britain. However, subsequent progress in high-resolution stratigraphy and correlations revealed serious flaws in many of these early stratotypes. During its Field Meeting held in Ludlow, UK, in 2011, the International Subcommission on Silurian Stratigraphy (ISSS) visited most of the boundary stratotypes of the Silurian series and stages (Davies *et al.* 2011b) and found that several of the GSSPs did not meet present requirements for resolution in global correlation. A unanimous decision was made to search for better GSSPs and either revise or replace the present, inadequate stratotypes. Three working groups have been formally established by the ISSS and have already commenced the search for new basal stratotypes of the Aeronian and Telychian stages of the Llandovery Series and the Sheinwoodian Stage of the Wenlock Series. A formal revision of the biostratigraphical definition of the GSSP for the base of the Rhuddanian Stage (also the base of the Llandovery Series and the Silurian System) has already previously been completed and formally approved (Rong *et al.* 2008).

Global correlation of Silurian rocks relies primarily on planktonic graptolites, supplemented by organic-walled microfossils (namely chitinozoans), as well as conodonts, which are usually confined to limestone successions. Biostratigraphical correlation has been reinforced by chemostratigraphy, particularly carbon isotope chemostratigraphy (e.g. Melchin & Holmden 2006; Cramer *et al.* 2011). Planktonic graptolites are the most common and

DOI 10.1111/let.12250

stratigraphically important fossils to be found in anoxic black shales, which are very widespread in Rhuddanian and Aeronian sedimentary successions worldwide. It has been hypothesized that black-shale sedimentation resulted from Hirnantian deglaciation of the Southern Hemisphere, coupled with global warming, rapid rise of sea level and temporary reduction in rates of oceanic circulation (Melchin *et al.* 2013). At that time, black, graptolitic shales indicative of low-oxygen bottom-water conditions spread globally over all latitudes and a wide range of water depths, whereas limestone deposition was confined to the shallower, inshore portions of deeply flooded shelves and platforms. Although the lowermost Silurian strata – Rhuddanian and Aeronian – have been recognized in many Palaeozoic terrains over the globe, readily accessible Rhuddanian–Aeronian boundary sections that do not show a break in sedimentation or notable lithological change that are also rich in well-preserved graptolites are relatively few and, for the most part, limited to Europe and China. Largely uninterrupted offshore black-shale successions with prolific planktonic graptolites are particularly widespread in the lower Silurian of peri-Gondwanan Europe. We focussed on the correlative potential of the Rhuddanian–Aeronian boundary sections in the classic lower Palaeozoic succession of the Prague Synform in the Barrandian area of Central Bohemia, Czech Republic. Rhuddanian and Aeronian sections of this terrain were studied for stratigraphical purposes by Bouček (1953) and Štorch (1986, 1994, 2006). The Hlásná Třebaň section, which best meets the formal requirements for a boundary stratotype (see Salvador 1994), is described herein in detail and proposed as a replacement for current Aeronian GSSP at the Trefawr track cutting. Graptolite biostratigraphy was integrated with a detailed lithological log and a variety of geochemical and rock magnetic proxies to assess the depositional and palaeoredox conditions and palaeoproductivity through the broad Rhuddanian–Aeronian boundary interval.

Present GSSP of the Aeronian Stage

The Aeronian was first defined as a stage by Cocks *et al.* (1984) who derived the name from Cwm-coed-Aeron Farm located ca. 500 m from the base Aeronian GSSP in the Trefawr track cutting in the northern part of the type Llandovery area of Wales. The Rhuddanian–Aeronian boundary occurs within the Cefngarreg Sandstone, a ca. 25-m-thick tongue of muddy sandstones within the Trefawr Formation (Cocks *et al.* 1984; Davies *et al.* 2011a). Uncommon graptolites allow for tentative recognition of the *Pernerograptus revolutus* (or *Coronograptus cyphus*), *Demirastrites triangulatus* (including our *Demirastrites pectinatus*) and *Neodiplograptus magnus* Biozone assemblages. Along with graptolites, the chitinozoans of the *Spinachitina maennili* Biozone are represented, and brachiopods and other shelly fossils, as well as acritarchs, occur at scattered levels throughout the section.

The base of the Aeronian Stage was defined 91 m above the base of the Trefawr Formation (Temple 1988) at a level marked with the appearance of the *triangulatus* Biozone graptolite fauna, represented by the occurrence of *Monograptus* (now *Pernerograptus*) *austerus sequens* (Hutt 1974). The taxon, however, is confined in a single sample level in the stratotype section. The highest evidence of the underlying Rhuddanian *cyphus* Biozone is provided by *Pernerograptus austerus vulgaris* (Hutt 1974) found 18 m below the boundary 'golden spike'. Temple (1988) called attention to faunal distribution at Trefawr track cutting, considering it inadequate to justify selection of the stage boundary stratotype at this section. Moreover, Zalasiewicz *et al.* (2009) restricted the stratigraphical range of *P. austerus sequens* to the middle part of the *triangulatus* Biozone. Thus, the current base of the Aeronian Stage most likely lies within the *triangulatus* Biozone, but probably not at the base of the Biozone, as was intended in the original concept of the GSSP level, and as it is currently used as a tool of global correlation (Melchin *et al.* 2012; Davies *et al.* 2013). The nominal index-species for the *triangulatus* Biozone has not been reported from the stratotype section, although it was questionably identified from the same stratigraphical level along a nearby transect (Cocks *et al.* 1984). In addition, *P. austerus sequens* is difficult to identify and has only been previously recorded outside of Great Britain by Bjerreskov (1975) from the island of Bornholm, Denmark, also from the middle portion of the *triangulatus* Biozone.

As the original concept of the base of the Aeronian Stage was intended to correspond to the base of the *triangulatus* Biozone, the first appearance datum (FAD) of *D. triangulatus* should be retained as the primary marker horizon at the GSSP for global correlation of the base Aeronian to respect the stability of the stage boundary. The base of the *triangulatus* Biozone has been widely adopted as a marker in global correlation (Zalasiewicz *et al.* 2009; Loydell 2012; Melchin *et al.* 2012). The utility of this definition is discussed herein, but other potential correlation tools for the Aeronian base, such as a positive shift in $\delta^{13}C_{org}$ just above the base (Melchin & Holmden 2006), are also considered. The Silurian was a time of relatively low faunal provincionalism among graptolites (Goldman *et al.* 2013), but some differences in graptolite ranges and faunal assemblages between distant areas have been known since the preliminary assessment by Melchin (1989). The new stratotype should be found in an area with a similar faunal affinity to the original stratotype area (Welsh Basin) in order to further support the stability of the Aeronian Stage concept.

Geological setting: Rhuddanian and Aeronian in the Prague Synform

The Palaeozoic of the Barrandian area represents the sedimentary cover of the Teplá–Barrandian Unit, considered by some authors to represent an independent microplate named Perunica (Havlíček *et al.* 1994; Fatka & Mergl 2009), which was detached from northwestern Gondwana, separate and distant from eastern Cadomian-type terranes (Linnemann *et al.* 2004; Murphy *et al.* 2006). In this interpretation, Perunica had remained close to Gondwana until the late Silurian (Cocks & Torsvik 2002, 2006; Torsvik & Cocks 2013). Another palaeogeographical concept considered the Teplá-Barrandian Unit as a part of the Armorican Terrane assemblage or HUN superterrane, which was an integral part of Gondwana until the late Silurian (Stampfli *et al.* 2002; Robardet 2003; von Raumer & Stampfli 2008). The palaeogeographical position of Perunica (e.g. of the Teplá-Barrandian Unit) within the Rheic Ocean is uncertain due to its apparent faunal affinities with different palaeocontinents (Ebbestad *et al.* 2013; Eriksson *et al.* 2013; Goldman *et al.* 2013; Kröger 2013; Meidla *et al.* 2013; Molyneux *et al.* 2013) and the wide range of palaeolatitudes proposed by palaeomagnetic studies (Tait *et al.* 1994, 1995; Krs & Pruner 1995, 1999; Krs *et al.* 2001; Patočka *et al.* 2003; Aïfa *et al.* 2007; Tasáryová *et al.* 2014).

Silurian rocks are preserved in the Prague Synform – a structure formed during the Variscan Orogeny (Fig. 1) – representing an erosional remnant of

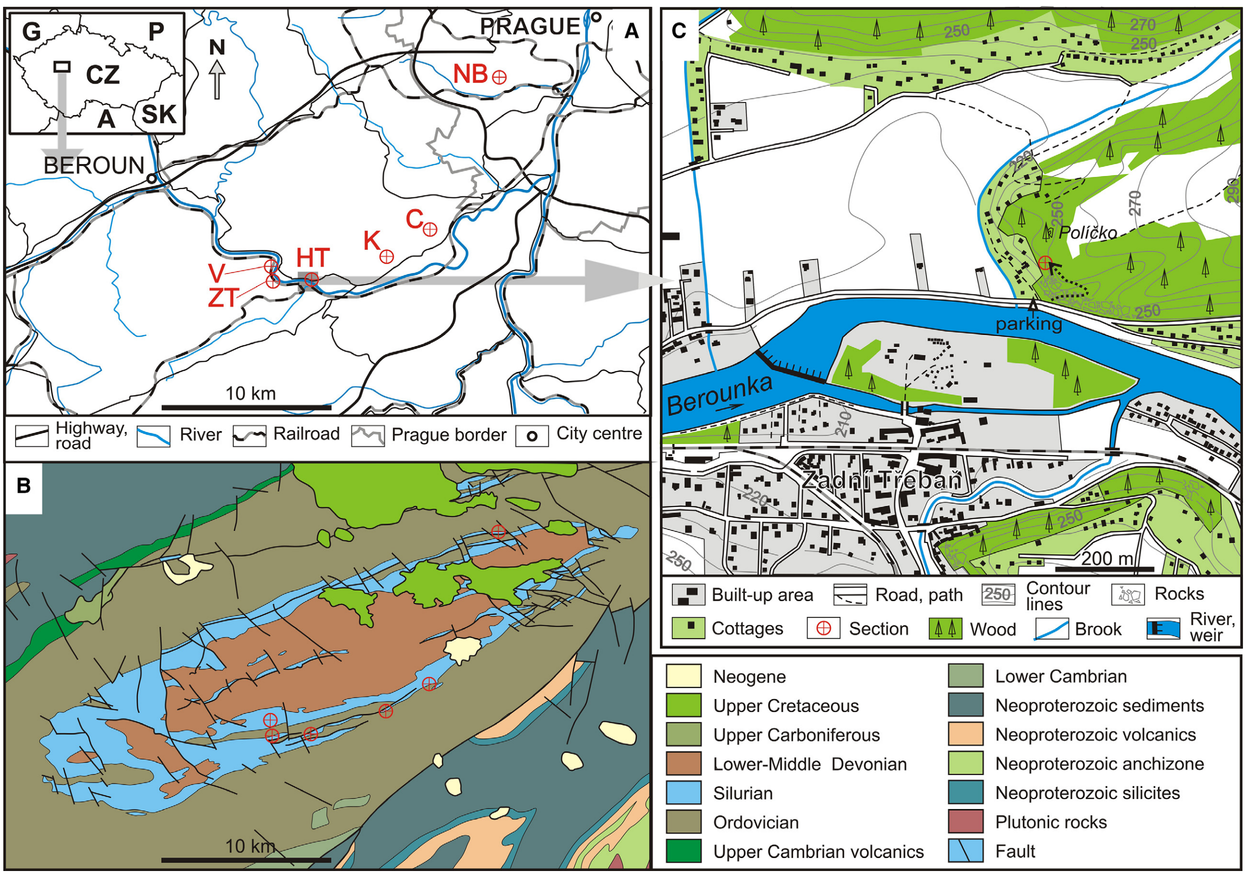

Fig. 1. Location maps: A, Location of the Hlásná Třebaň section (HT) and the location of five auxiliary reference sections with the Rhuddanian–Aeronian boundary strata; Karlík section (K), Černošice section (C), Zadní Třebaň section (ZT), Vočkov section (V) and Nové Butovice section (NB). Small inset shows generalized location of the study area in central Europe (CZ – Czech Republic, SK – Slovakia, G – Germany, A – Austria, P – Poland). B, simplified geological map the Prague Synform showing the same territory and sections as map A. C, detailed location of the Hlásná Třebaň section.

a continental rift basin called the Prague Basin by some authors, infilled by an Ordovician to Middle Devonian marine sedimentary succession and associated basaltic volcanic rocks (for a summary see Chlupáč *et al.* 1998).

In the Prague Synform, both the Rhuddanian and Aeronian stages are represented by the Želkovice Formation, comprising an 8-m-thick to 12-m-thick, condensed offshore marine, anoxic sedimentary succession (Kříž 1998). Black silty shales, siliceous shales and thin-bedded silty silicites (coarsely laminated shale enriched in ?biogenic silica and silica remobilized from fine quartz silt) predominate, whereas clayey shales are confined to the lowermost part of the Želkovice Formation (Štorch 2006). The strata are rich in a nearly cosmopolitan graptolite fauna (Bouček 1953; Štorch 1994) associated with organic-walled microfossils (Dufka *et al.* 1995). Graptolites, in particular, have been used as an effective tool for long-range correlation with high precision. Shelly faunas are very rare. The lowermost part of the formation yielded some indeterminable 'orthid' brachiopods (Bouček 1953); minute 'inarticulate' brachiopods are locally common in the uppermost part of the formation, and cephalopod opercula of *Discinocaris* and *Plectocaris* occur rarely throughout the formation (for summary see Kříž 1998). Very rare specimens of the nautiloid *Discoceras*, with a coiled shell, occur in the earliest Aeronian strata (Š. Manda and V. Turek, unpublished data, 2016).

The Želkovice Formation overlies pale-coloured uppermost Hirnantian mudstones of the Kosov Formation. The onset of anoxic black-shale sedimentation coincided almost precisely with the base of the lowermost Silurian *Akidograptus ascensus* Biozone (Horný 1956; Štorch 1986). Sedimentation temporarily ceased in the lower Rhuddanian, resumed in the upper part of the *Cystograptus vesiculosus* Biozone in the majority of studied sections (Fig. 2), and continued apparently without interruption across the Rhuddanian–Aeronian boundary interval through the entire Aeronian until deposition of unfossiliferous beds of pale-coloured mudstone and

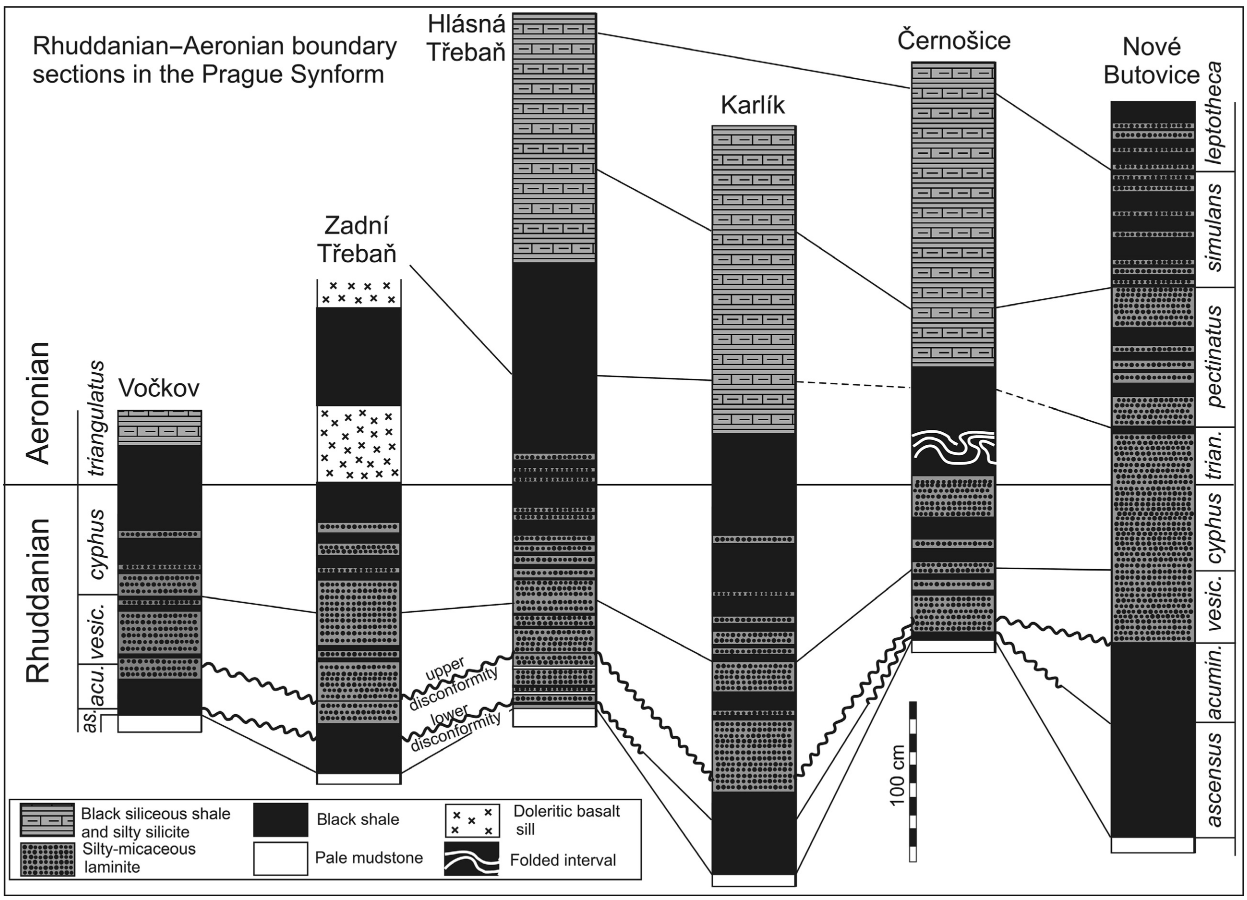

Fig. 2. Correlation of Rhuddanian–Aeronian sections exposed in the southern limb and northeastern limb of the Prague Synform. Simplified section logs after Štorch (1986), revised and updated. Abbreviations: *as.* – *ascensus* Biozone; *acu.*, *acumin.* – *acuminatus* Biozone; *vesic.* – *vesiculosus* Biozone; *trian.* – *triangulatus* Biozone.

claystone marks the base of succeeding Litohlavy Formation of Telychian age (Kříž 1975; Štorch 2006; Štorch & Frýda 2012). The most complete black-shale successions, with the fewest and most minimal gaps in sedimentation, are developed in southwestern and northeasternmost parts of the Prague Synform. In contrast, there is a long-lasting break in the sedimentary record comprising the whole Rhuddanian, Aeronian and also early Telychian that is recognized in an area confined to the north-central part of the Prague Synform (Štorch 1986, 2006). In many sections, the lower Silurian black-shale succession is sandwiched by alkaline doleritic basalt sills (Kříž 1998). The subsequent Variscan Orogeny affected the Želkovice Formation only slightly as demonstrated by minor and local folding, subordinate faulting (Kříž 1998) and low-to-moderate thermal maturity in the range of 90–180 °C (Suchý *et al.* 2002).

Rhuddanian–Aeronian boundary sections of the Prague Synform

Based on earlier stratigraphical studies devoted to the Llandovery strata of the Barrandian area and their correlation with other European regions (Bouček 1953; Štorch 1986, 2006), six localities qualified for closer examination of the Rhuddanian–Aeronian boundary strata: Hlásná Třebaň, Karlík, Vočkov, Zadní Třebaň, Černošice and Nové Butovice (Figs 1, 2). All sections exhibit similar sedimentary successions across the Rhuddanian–Aeronian boundary. Minor differences were found in thickness, facies details and extent of unconformities. In addition, the graptolite succession is almost identical in all of the sections, except for minor differences that result from artefacts of preservation and sampling biases, coupled with lithological development, weathering and the thermal effects of neighbouring basalt sills.

Hlásná Třebaň section. – The section crops out on the hillside high above the road from Hlásná Třebaň to Lety (Fig. 3A) on the left bank of Berounka River (GPS coordinates: 49°55′22.93″N, 14°12′42.97″E; Fig. 1). The Hirnantian sedimentary succession, exposed above a massive sill of Silurian doleritic basalt, starts with silty shales of the middle part of the Kosov Formation. In the middle of the hillslope, storm-dominated marine shelf sandstones of the upper Kosov Formation rest on the shaly succession with a prominent erosional unconformity (Brenchley & Štorch 1989; Štorch 2006). Several pulses of clast-supported conglomerates with sandstone matrix infilled a shallow channel incised

Fig. 3. Hlásná Třebaň Section – field photographs. A, Rhuddanian and lower Aeronian black shales cropping out downslope of the sampled exposure. Red bar indicates the base of the Aeronian Stage. B, Sampled section after first round of sampling. Red line marks the base of the *triangulatus* graptolite Biozone and proposed Rhuddanian–Aeronian boundary. C, Rhuddanian–Aeronian boundary beds in detail.

unconformably into the soft shale. Conglomerates are overlain by packets of coarse, upward-fining sandstone beds with rip-up clasts, internal erosion surfaces and hummocky cross-stratification. Wave ripples and hummocky cross-stratification are also developed in succeeding couplets of fine-grained sandstones and silty-micaceous shale. The upward-fining sequence near the top of the Kosov Formation is interpreted to represent the late Hirnantian post-glacial rise in sea level (Brenchley & Štorch 1989; Štorch 2006).

The Ordovician–Silurian boundary is exposed a few metres below the upper hillslope edge. It is marked by an abrupt change from yellowish, bioturbated clay mudstone of the topmost Kosov Formation to black shale of the lowermost Želkovice Formation with graptolites of the basal Silurian *Akidograptus ascensus* Biozone. Rhuddanian sedimentation, dominated by graptolite-rich black silty-micaceous laminites, was interrupted by two discrete unconformities (Figs 2, 4). The upper *ascensus* and/or lowermost *Parakidograptus acuminatus* biozones are missing at the lower disconformity and the upper *acuminatus* and lower *Cystograptus vesiculosus* biozones are missing at the upper disconformity. The overlying, uninterrupted black-shale succession begins in the upper *vesiculosus* Biozone and continues through the *Coronograptus cyphus* Biozone, across the Rhuddanian–Aeronian boundary, through the *Demirastrites triangulatus* Biozone, *Demirastrites pectinatus* Biozone, *Demirastrites simulans* Biozone and *Pribylograptus leptotheca* Biozone, terminating in the middle of the Aeronian *Lituigraptus convolutus* Biozone, which is slightly thermally altered by an overlying basalt sill.

Karlík section. – This is a shallow excavation at the top of a wooded hill northeast of the village of Karlík (49°56′30.02″N, 14°16′8.58″E, Fig. 1), which exhibits a fairly uninterrupted succession of the *ascensus* and lower and middle *acuminatus* biozones. The upper *vesiculosus* Biozone, above the middle Rhuddanian disconformity, is duplicated by a local thrust-fault. Thickness, lithology and graptolite assemblages are nearly identical to those at Hlásná Třebaň. The upper part of the succession, beginning with the upper *pectinatus* Biozone, is markedly thermally altered by an overlying doleritic basalt sill.

Voćkov section. – The section, exposed by a shallow trench at the forested Voćkov Hill near Karlštejn (49°55′34.10″N, 14°10′53.60″E, Fig. 1), comprises the latest Hirnantian pale mudstone and Rhuddanian and early Aeronian black shales and silty-micaceous laminites. The upper *acuminatus* and lower *vesiculosus* biozones are missing due to a short gap in sedimentation. The section terminates in the middle of the *triangulatus* Biozone (Štorch 1986).

Zadní Třebaň section. – The section is exposed in a railroad cut 1.3 km west of the Zadní Třebaň railway station (49°55′10.48″N, 14°11′5.80″E, Fig. 1). The lithology, thicknesses, and middle Rhuddanian disconformity, associated with a short-term gap in sedimentation, are closely similar to those at the Voćkov section. However, the Rhuddanian–Aeronian boundary interval has been intruded and altered by a thin basalt sill, and black shales of the *triangulatus* Biozone are thermally altered by another, thicker basalt sill higher in the section (Štorch 1986).

Černošice section. – A shallow excavation exposes the uppermost Hirnantian pale mudstone and Rhuddanian–Aeronian black-shale succession on a wooded hillslope above the road from Černošice to Solopysky (49°57′27.06″N, 14°18′22.98″E, Fig. 1). The steeply dipping black shale is folded immediately above the base of the Aeronian *triangulatus* Biozone. Two gaps in sedimentation occur in the lower and middle Rhuddanian part of the succession. The upper *ascensus* and lower *acuminatus* biozones are missing at the lower disconformity, and omission of the upper *acuminatus* and lower *vesiculosus* biozones marks the upper disconformity. The *pectinatus*, *simulans* and *leptotheca* biozones are particularly rich in well-preserved graptolites.

Nové Butovice section. – Temporary building excavations in Prague-Nové Butovice (50°2′51.11″N, 14°20′37.53″E, Fig. 1) exposed the Hirnantian–Telychian succession (Štorch 2006; fig. 5), which is significant for the occurrence of the *Hirnantia* fauna of shelly fossils and the Hirnantian zonal index graptolite *Metabolograptus persculptus* (Elles & Wood 1907) in the uppermost Kosov Formation. The Želkovice Formation consists of relatively thick black shales of the lower Rhuddanian *ascensus* and lower *acuminatus* biozones. Higher up in the succession there is a short gap in sedimentation that corresponds to the upper *acuminatus* and lower *vesiculosus* biozones. Silty-micaceous laminites predominate above that break extending from the middle Rhuddanian to middle Aeronian.

Of the sections listed above, the Hlásná Třebaň section (Figs 2–4) exhibits the most complete, easily accessible, and least thermally and tectonically affected Rhuddanian–Aeronian sedimentary succession with continuous and monotonous sedimentation across the boundary interval in the Prague Synform. The section has yielded abundant, diverse, and usually well-preserved graptolites, identifiable chitinozoans, and a carbon and nitrogen isotope record that appears to preserve primary values. It is described below as a new candidate for the GSSP of the Aeronian Stage.

The locality was briefly described for the first time by Kodym *et al.* (1931) and then by Přibyl (1937). A

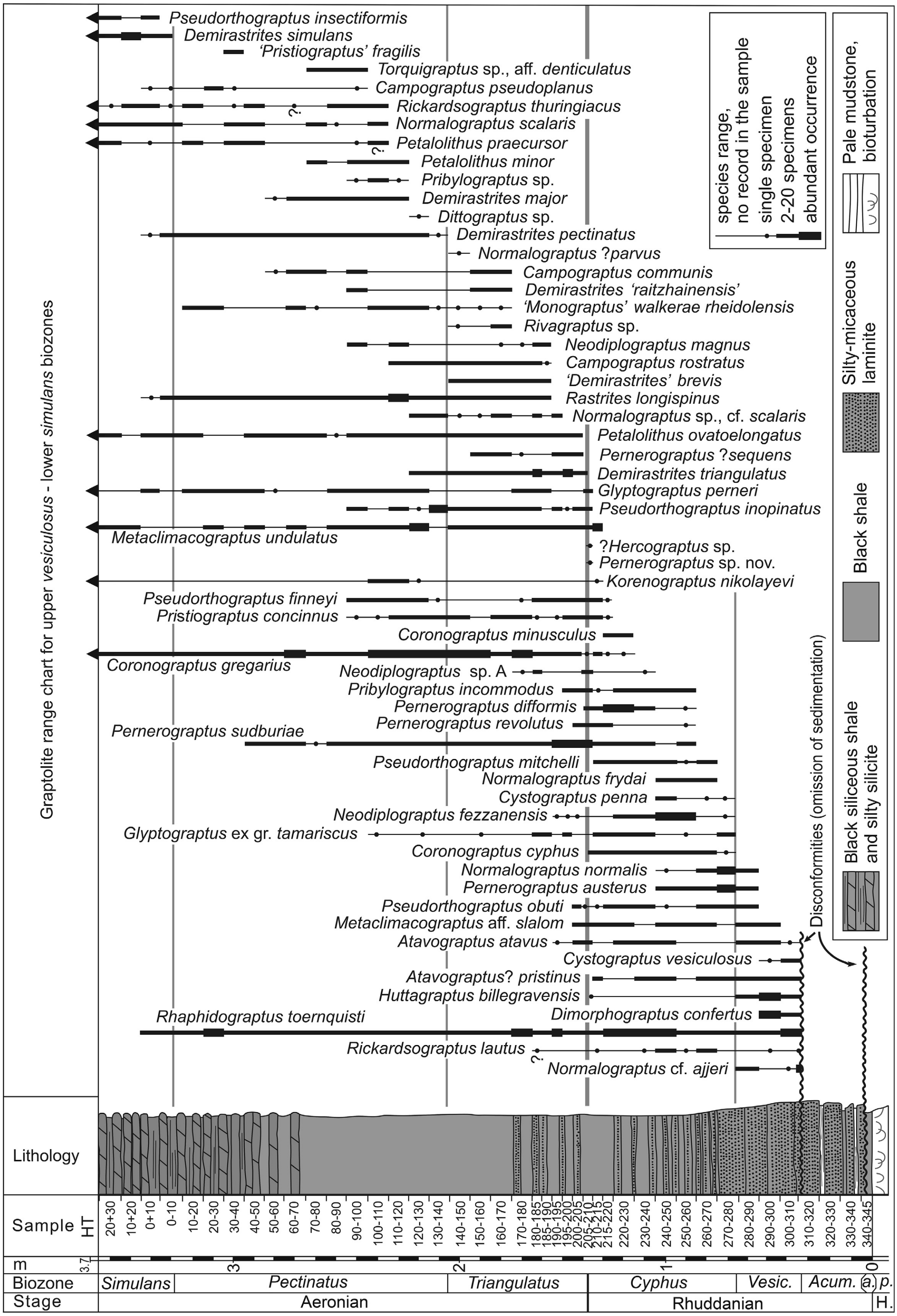

Fig. 4. Stratigraphy, lithology, sampling intervals and graptolite range chart of the Rhuddanian–Aeronian Hlásná Třebaň section. Abbreviations: *vesic.* – *vesiculosus* Biozone, *acum.* – *acuminatus* Biozone, *a.* – *ascensus* Biozone, *p.* – *Metabolograptus persculptus* Biozone, H – Hirnantian.

more detailed description and full list of reference was provided by Kříž (1992), including a tentative log and a graptolite range chart of the Rhuddanian and Aeronian strata based upon the unpublished thesis by Štorch (1991). Štorch (2006) published a generalized sedimentary log that also included the Hirnantian sequence. Chitinozoan and acritarch data from the uppermost Hirnantian and Rhuddanian strata were discussed by Dufka & Fatka (1993). Chitinozoans are moderately common and determinable, acritarchs are rare except for a rich assemblage isolated by Dufka & Fatka (1993) from a thin, pale-coloured bed in the *acuminatus* Biozone, 24 cm above the base of the black-shale succession. Frýda & Štorch (2014) published the first data on the C_{org} isotope and TOC compositions from the Hlásná Třebáň section, covering the stratigraphical interval from the Ordovician–Silurian boundary to the *convolutus* Biozone.

Methods

The section, which has been repeatedly studied by PŠ since 1979, was measured and then systematically sampled by PŠ, ŠM, JF, ZT and LC in 2013, 2014 and 2015 for its fossil record (graptolites, chitinozoans), lithology, geochemistry (organic carbon, carbon and nitrogen isotopes, whole-rock composition) and magnetic susceptibility.

Fossil record and biostratigraphy

Particular attention has been focussed on the rich, high-diversity graptolite assemblages preserved on almost every bedding plane that occur throughout the black-shale succession. Each 10-cm-thick interval of the section was sampled in two rounds, and every graptolite, at least tentatively identifiable, was collected from a sampled rock volume of ca. 0.02 m^3 for each interval. Finer sampling intervals, 5 cm thick, and ca. 0.01 m^3 rock volumes were collected and studied in Rhuddanian–Aeronian boundary strata (Fig. 4). Graptolite collections comprised about 5000 specimens representing 65 species from the *ascensus*–lowermost *simulans* biozones. Fifty-nine species were identified in the upper *vesiculosus*–lowermost *simulans* biozones, including 30 taxa recorded for the first time in the Hlásná Třebaň section, despite earlier systematic studies by Přibyl (1941, 1942), Přibyl & Münch (1941), Bouček & Přibyl (1942), Bouček (1944) and Štorch (1983, 1985, 1988), which were devoted to selected graptolite genera of the Barrandian lower and middle Llandovery. The present taxonomic re-evaluation benefits from recent study of the rich, stratigraphically coeval material of particularly well-preserved graptolites from loose blocks of bleached shale collected near the village of Všeradice (Štorch 2015).

Black shales and silty silicites yield flattened graptolite rhabdosomes without any sign of tectonic strain. Rhabdosomes that commonly are preserved with high-reflectance, in partly pyritized organic matter exhibit considerable thecal details, long spines, unbroken virgellae and nemata. Bedding planes of silty-micaceous laminites are crowded by less well-preserved, largely biserial specimens.

The graptolite material from this study is housed with the Czech Geological Survey, Prague, in collections prefixed PŠ. The section was also sampled for organic-walled microfossils at the same regular intervals as the graptolites (10 cm and 5 cm) from the Silurian–Ordovician boundary to base of the *simulans* Biozone. The samples were given to Anthony Butcher (University of Portsmouth) for study.

Lithology

Here, we present results of our study of lithology and whole-rock elemental geochemistry based upon 18 shale samples spanning the entire section at Hlásná Třebaň, collected at an interval of 20 cm. The lithofacies samples were studied using thin sections and the TESCAN Vega scanning electron microscope equipped with an X-Max 50 (Oxford Instruments) EDS detector at the Faculty of Science, Charles University, Prague.

Whole-rock elemental geochemistry

Representative ca. 50 g samples were collected from the same levels as those for lithology, powdered and analysed for selected major and trace elements in laboratories at the Institute of Geology of the CAS, v. v. i., (Department of Geological Processes, Department of Environmental Geology and Geochemistry). Major elements were determined using an Agilent 5100 SVDV ICP-OES inductively coupled plasma optical emission spectrometer. Trace elements (transition metals, rare earth and selected large ion lithophile elements) were measured using an ELEMENT 2 (ThermoFisher Scientific) inductively coupled plasma mass spectrometer. Geochemical data were processed using *GCDkit* (Janoušek *et al.* 2006). Cerium (Ce/Ce*) and europium (Eu/Eu*) anomalies were calculated from: $[Ce/Ce^*]_{PAAS} = Ce_N/(La_N \times Pr_N)^{1/2}$ and $[Eu/Eu^*]_{PAAS} = Eu_N/(Sm_N \times Gd_N)^{1/2}$ (PAAS – Post Archaean Australian Shale; Taylor & McLennan 1985). Authenticity of the Ce anomalies was verified by calculation of praseodymium ratios $[(Pr/Pr^*)_{PAAS} = Pr_N/(0.5Ce_N + 0.5Nd_N)]$ following Bau & Dulski (1996). The studied interval included samples from all biozones except *ascensus*: two from *acuminatus*, two from *vesiculosus*, three from *cyphus*, four from *triangulatus*, six from *pectinatus* and one from the *simulans* Biozone. Analytical data are provided in Table S1.

Carbon and nitrogen isotope geochemistry and total organic carbon

The section was densely sampled for total organic carbon content (TOC) and for organic carbon and bulk nitrogen isotope composition using the same intervals as the biostratigraphical samples (10 cm) from the Ordovician–Silurian boundary to base of the *simulans* Biozone. This was done to increase the resolution of the record relative to the previous sampling of a stratigraphically wider range from this section (from the Ordovician–Silurian boundary to the *convolutus* Biozone) presented by Frýda & Štorch (2014). The new sampling (Fig. 4) includes 37 samples for whole-rock nitrogen and organic carbon isotope composition and TOC. Analytical data are provided in Table S2. Hand specimens were cut, and rock powder was prepared from a few grams of a fresh sample. A few milligrams of rock powder was taken for TOC and isotope analyses. Before analyses, rock powders were decarbonatized even though their calcium carbonate content was $\ll 1$ wt. %, then washed and dried. About 20 mg of rock powder was used for TOC and about 10 mg for carbon and nitrogen isotope analyses. Samples were combusted in a Fisons 1108 elemental analyser coupled online to a Finnigan Mat 251 mass spectrometer via a ConFlo interface. As reference material, NBS 22 (Gulf oil, with $\delta^{13}C$ value $-29.75‰$ VPDB), acetanilid (Analytical Microanalysis, UK), IAEA N-1 (with $\delta^{15}N$ value 0.4‰), IAEA N-2 (with $\delta^{15}N$ value 20.3‰) and a laboratory standard $(NH_4)_2SO_4$ (with $\delta^{15}N$ value $-1.7‰$) were measured. Accuracy and precision were controlled by replicate measurements of laboratory standards and were better than $\pm 0.1‰$ (1σ) for organic carbon isotope composition, better than $\pm 0.3‰$ (1σ) for nitrogen isotope composition and better than $\pm 0.02\%$ (1σ) for TOC content. Isotope trend lines were calculated using the nonparametric locally weighted regression method 'Locfit' (Loader 1999), which produces a 'smoothed' curve retaining the local minima and maxima. The nonparametric Mann–Kendall test was used to detect statistically significant monotonic trends in series of measured data (Mann 1945; Kendall 1975).

Magnetic susceptibility

A total of 76 whole-rock samples were collected from the section at 5 cm vertical intervals for magnetic susceptibility (MS) study. Samples were cleaned, and residues were removed from the surface. MS measurements were made on rock samples with an average weight of 33 g. Mass-specific MS measurements, expressed in $10^{-9} \times m^3/kg$, were made using a MFK1-FA Kappabridge (Agico Inc., Brno) at a magnetic field of 200 Am-1.

Results and interpretation

Fossil record and biostratigraphy

The Silurian succession (Fig. 4) begins with an abrupt change from yellowish, bioturbated mudstones of the Hirnantian Kosov Formation to fine black shales of the lowermost Želkovice Formation, with graptolites of the basal Silurian *ascensus* Biozone, in particular *Neodiplograptus lanceolatus* Štorch & Serpagli 1993; and *A. ascensus* Davies 1929. The lowermost black-shale interval, which is less than 5 cm thick, is separated by a disconformity from the overlying black silty-micaceous laminites (Fig. 4) with graptolites of the middle *acuminatus* Biozone: *P. acuminatus* (Nicholson 1867), *A. ascensus*, *Neodiplograptus apographon* (Štorch 1983), *N. lanceolatus*, *Cystograptus ancestralis* Štorch 1985; *Normalograptus longifilis* (Manck 1923) and *Normalograptus* cf. *ajjeri* (Legrand 1977). This assemblage was discussed in a broader biostratigraphical and palaeobiogeographical context by Štorch (1996), and the species are not listed in the range chart on Figure 4. Well-preserved graptolites are confined to fine black shales that are associated with a 2-cm-thick grey mudstone without graptolites, 22 cm above the base of the black-shale succession.

The upper *acuminatus* and lower *vesiculosus* biozones are missing due to another disconformity developed across the basin. The latter disconformity separates the middle *acuminatus* Biozone from silty-micaceous laminites crowded with poorly preserved graptolites indicating the upper part of the *vesiculosus* Biozone. *Dimorphograptus confertus* (Nicholson 1868a), *Rhaphidograptus toernquisti* (Elles & Wood 1906), *Huttagraptus billegravensis* Koren' & Bjerreskov 1997; *Atavograptus atavus* (Jones 1909), *Atavograptus*? *pristinus* (Hutt 1975) and *Metaclimacograptus* aff. *slalom* Zalasiewicz 1996 have been recognized in this 33-cm-thick interval along with the zonal index, *Cystograptus vesiculosus* (Nicholson

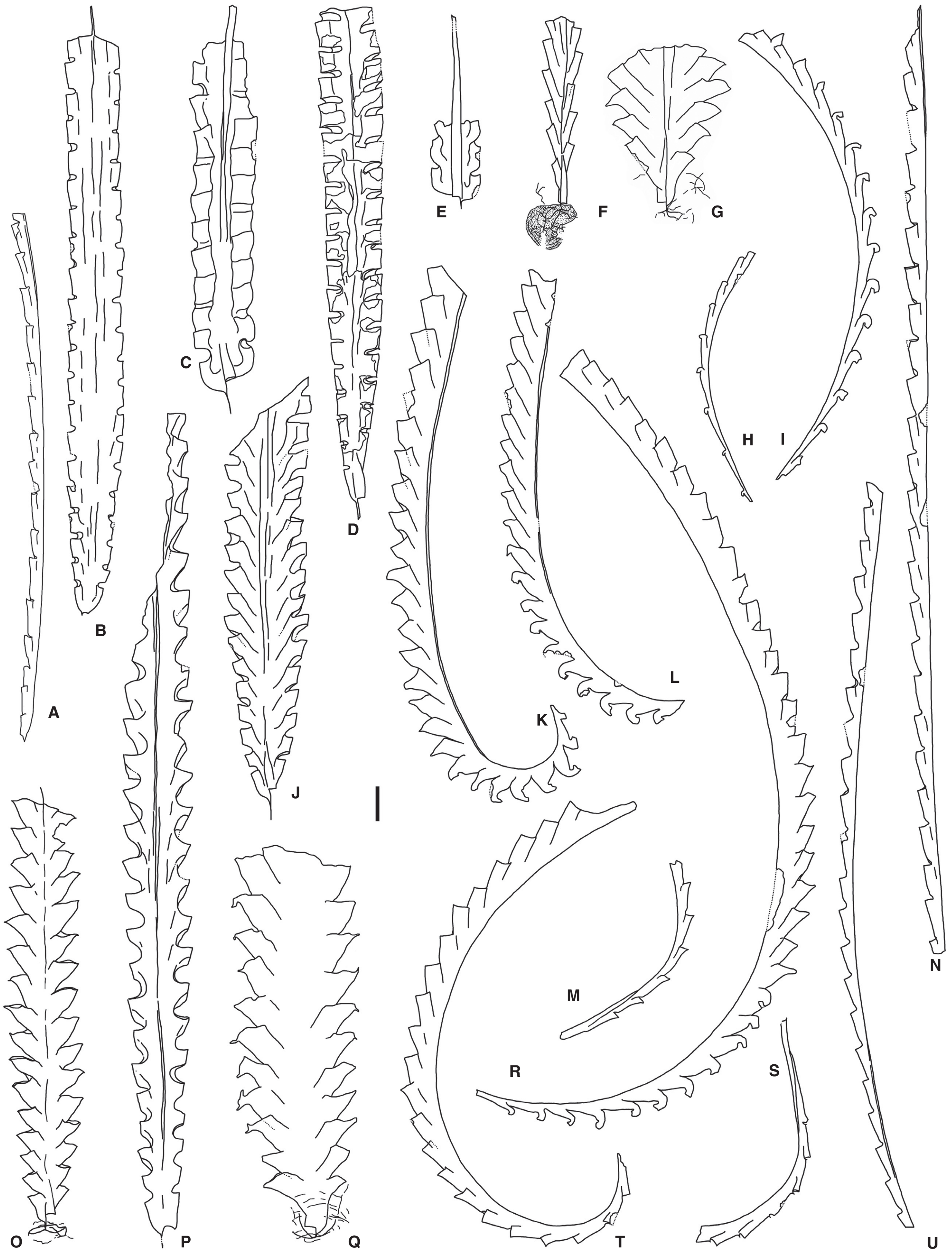
A
B
C
D
E
F
G
H
I
J
K
L
M
N
O
P
Q
R
S
T
U

Fig. 5. Graptolite fauna of the upper Rhuddanian *Coronograptus cyphus* Biozone – selected taxa. A, *Pribylograptus incommodus* (Törnquist 1899), PŠ 4083, mesial fragment from sample HT207–210. B, *Normalograptus frydai* Štorch 2015, PŠ 3563 from the lower part of the biozone. C, E, *Cystograptus penna* (Hopkinson 1869), C, PŠ 3428, middle part of the biozone. E, PŠ 3964, juvenile rhabdosome from sample HT240–250. D, *Rhaphidograptus toernquisti* (Elles & Wood 1906), PŠ 3964, sample HT240–250. F, *Pseudorthograptus finneyi* Štorch & Kraft 2009, PŠ 3945, sample HT205–210. G, Q, *Pseudorthograptus obuti* (Rickards & Koren' 1974). G. PŠ 4142, sample HT207–210. Q, PŠ 3462, upper part of the biozone. H, *Pernerograptus sudburiae* (Hutt 1974), PŠ 4006, mesial fragment from sample HT220–230. I, *Pernerograptus revolutus* (Kurck 1882), PŠ 3914, mesial fragment from sample HT210–215. J, *Neodiplograptus fezzanensis* (Desio 1940), PŠ 4013/3, sample HT240–250. K, *Pernerograptus* sp. nov., PŠ 3965, sample HT207–210. L, R, *Pernerograptus difformis* (Törnquist 1899); L. PŠ 4280, mesial part from the uppermost part of the biozone, R. PŠ 3961, sample HT207–210. M. *Coronograptus minusculus* Obut & Sobolevskaya, 1968, PŠ 3919, sample HT207–210. N, U, *Atavograptus atavus* (Jones 1909). N, PŠ 4088, distal fragment from sample HT207–210. U, PŠ 4109, sub-proximal part from sample HT220–230. O, *Pseudorthograptus mitchelli* Štorch 2015, PŠ 3915, sample HT220–230. P, *Korenograptus nikolayevi* (Obut 1965), PŠ 3953, sample HT210–215. S, T, *Coronograptus cyphus* (Lapworth 1876). S, PŠ 4279/2, proximal part from the middle part of the biozone. T, PŠ 3950, sample HT210–215. A, D, K, M, P, R, T, U from the Hlásná Třebaň Section (HT); B, C, L, Q, S from Všeradice described by Štorch (2015). Scale bar represents 1 mm.

1868b), and some largely unidentifiable normalograptids and metaclimacograptids.

The *cyphus* Biozone comprises a 0.73-m-thick interval of silty-micaceous laminites passing upward into thin-bedded shale with subordinate silty-micaceous laminae. It is the interval between the lowest occurrence of *C. cyphus* (Lapworth 1876) and the lowest occurrence of *Demirastrites triangulatus* (Harkness 1851). The latter almost precisely coincides with the highest occurrence of *C. cyphus*. The name-giving taxon (Fig. 5S, T) is moderately common through the whole *cyphus* Biozone. The graptolite taxa that appear in the lower part of the Biozone also include *Neodiplograptus fezzanensis* (Desio 1940) (Fig. 5J), *Pseudorthograptus obuti* (Rickards & Koren' 1974) (Fig. 5G, Q), *Normalograptus frydai* Štorch 2015 (Fig. 5B), *Pernerograptus austerus* (Törnquist 1899), *Cystograptus penna* (Hopkinson 1869) (Fig. 5C, E), *Pseudorthograptus mitchelli* Štorch 2015 (Fig. 5O), *Glyptograptus* ex gr. *tamariscus* (Nicholson 1868a) and abundant specimens of *Rhaphidograptus toernquisti* (Fig. 5D). *Pribylograptus incommodus* (Törnquist 1899) (Fig. 5A), *Pernerograptus sudburiae* (Hutt 1974) (Fig. 5H), uncommon occurrences of *Pernerograptus revolutus* (Kurck 1882) (Fig. 5I), and abundant specimens of *Pernerograptus difformis* (Törnquist 1899) (Fig. 5L, R) begin in the middle of the *cyphus* Biozone. *Coronograptus gregarius* (Lapworth 1876) and rare specimens of *Coronograptus minusculus* Obut & Sobolevskaya, 1968 (Fig. 5M) appear in the upper part of the *cyphus* Biozone, along with several other taxa (see Fig. 4). The upper two to three 5-cm-thick sample levels of the *cyphus* Biozone yielded the lowest occurrences of *Pristiograptus concinnus* (Lapworth 1876), *Metaclimacograptus undulatus* (Kurck 1882) and *Pseudorthograptus finneyi* Štorch & Kraft 2009 (Fig. 5F). *Pseudorthograptus inopinatus* (Bouček 1944) and *Glyptograptus perneri* Štorch 2015 appear only few centimetres below FAD of *Demirastrites triangulatus* (Harkness 1851). Also, a single specimen of *Pernerograptus* sp. nov. – an easily recognizable but as yet undescribed species (Fig. 5K) confined to the uppermost *cyphus* Biozone in Spain (P. Štorch, personal observation, 2015) – also came from this level.

Fine black shales with abundant and well-preserved graptolites (Fig. 6) occur across the

Fig. 6. Slab from the lower part of the *triangulatus* Biozone at Hlásná Třebaň Section (PŠ 4281, sample HT 190–195) showing graptolite assemblage dominated by the zonal index fossil *Demirastrites triangulatus* (Harkness). Scale bar represents 10 mm.

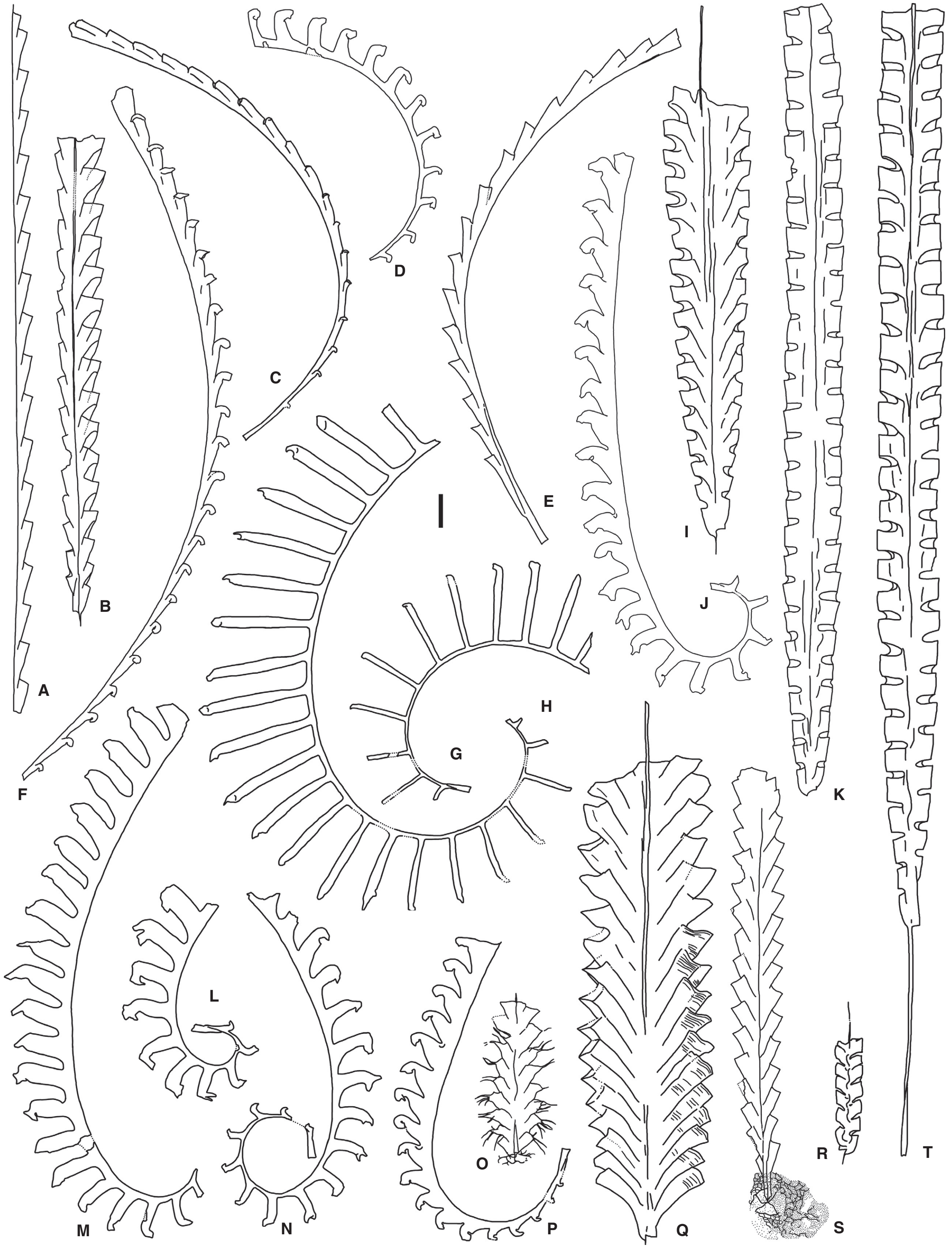
A
B
C
D
E
F
G
H
I
J
K
L
M
N
O
P
Q
R
S
T

Fig. 7. Graptolite fauna of the lowermost Aeronian *Demirastrites triangulatus* Biozone – selected taxa. A, *Pristiograptus concinnus* (Lapworth 1876), PŠ 3949, mesial part from sample HT180–190. B, *Glyptograptus perneri* Štorch 2015, PŠ 3943, sample HT205–207. C, *Pernerograptus sudburiae* (Hutt 1974), PŠ 3910b, sample HT200–205. D, *Demirastrites*? *brevis* (Sudbury 1958), PŠ 4162, sample HT180–185. E, *Coronograptus gregarius* (Lapworth 1876), PŠ 3922, sample HT 150–160. F, *Pernerograptus revolutus* (Kurck 1882), PŠ 3959, sample HT205–207. G, H, *Rastrites longispinus* Perner 1897. G, PŠ 4103a, sample HT140–150. H, PŠ 3954, sample HT160–170. I, *Neodiplograptus magnus* (H. Lapworth 1900), PŠ 3916, sample HT180–190. J, *Demirastrites*? *raitzhainensis* Eisel 1912, PŠ 3988a, sample HT160–170. K, *Normalograptus* sp., cf. *scalaris* (Hisinger 1837), PŠ 3956, sample HT185–190. L–N, *Demirastrites triangulatus* (Harkness 1851). L, PŠ 4219, sample HT195–200. M, PŠ 4220, sample HT195–200, N. PŠ 4224 early morphotype common in sample HT200–205. O, *Pseudorthograptus inopinatus* (Bouček 1944), PŠ 3923, sample HT205–207. P, *Campograptus rostratus* (Elles & Wood 1913), PŠ 3912, sample HT140–150. Q, *Petalolithus ovatoelongatus* (Kurck 1882), sample HT160–170. R, *Metaclimacograptus undulatus* (Kurck 1882), PŠ 4131, sample HT180–185. S, *Pseudorthograptus finneyi* Štorch & Kraft 2009, PŠ 3948, sample HT205–207. T, *Rhaphidograptus toernquisti* (Elles & Wood 1906), PŠ 4150, sample HT160–170. All specimens from the Hlásná Třebaň Section, scale bar represents 1 mm.

Rhuddanian–Aeronian boundary interval. The base of the Aeronian Stage is herein marked by the base of the *triangulatus* Biozone, defined by the lowest occurrence of the name-giving graptolite, *D. triangulatus* (Fig. 7L–N). Based on our detailed study, we believe that the material from Rheidol Gorge, Wales, described by Sudbury (1958) as *M. separatus separatus* Sudbury 1958 and *M. separatus triangulatus* (Harkness 1851), should both be regarded as synonymous with *D. triangulatus* (Harkness 1851), as represented in the Hlásná Třebaň section. Samples from the lowermost part of 0.67-m-thick *triangulatus* Biozone at Hlásná Třebaň show rapid graptolite diversification, including the successive appearance of several new lineages, including several groups of monograptids with isolated and hooked thecae (*Demirastrites, Rastrites* and *Campograptus*), as well as species of *Petalolithus*. As noted above, the appearance of *D. triangulatus* occurred closely above the lowest occurrences of *P. finneyi* (Fig. 7S), *P. inopinatus* (Fig. 7O), *M. undulatus* (Fig. 7R), *P. concinnus*, and the initial proliferation of *C. gregarius* (7E). *Petalolithus ovatoelongatus* (Kurck 1882) (Fig. 7Q) appeared in the first 5-cm-thick sample above the boundary stratum. In addition, *Rastrites longispinus* Perner 1897 (Fig. 7G, H), *Campograptus rostratus* (Elles & Wood 1913) (Fig. 7P), *Demirastrites brevis* (Sudbury 1958) (7D), and, surprisingly, *Neodiplograptus magnus* (Lapworth 1900) (7I), joined the assemblage in the lower part of the *triangulatus* Biozone, whereas *Campograptus communis* (Lapworth 1876), *Demirastrites* cf. *raitzhainensis* (Eisel 1912) *sensu* Elles & Wood (1913) (Fig. 7J) and '*Monograptus*' *walkerae rheidolensis* Rickards *et al.* 1977 appeared in the upper part of the Biozone. *Atavograptus*? *pristinus* and *C. cyphus* disappeared at the top of the *cyphus* Biozone and last specimens of *P. obuti* were found a few centimetres above the zonal boundary, at the level where *P. ovatoelongatus* made its lowest occurrence. *Neodiplograptus fezzanensis*, *A. atavus* (Fig. 5N, U), *P. revolutus, P. difformis* and *P. incommodus* have their highest occurrences in the lower part of the *triangulatus* Biozone. In total, 31 graptolite species have been found in the *triangulatus* Biozone of the Hlásná Třebaň section.

The diversification of triangulate monograptids continued through the succeeding *Demirastrites pectinatus* Biozone, which embraced a 1.34-m-thick interval. Along with the proliferation of *C. gregarius* (Fig. 8F) and *R. longispinus* (Fig. 8M), demirastritids further diversified, being represented by the zonal index *Demirastrites pectinatus* (Richter 1853) (Fig. 8K, P) [= *M. fimbriatus* (Nicholson 1868a)] and *Demirastrites major* (Elles & Wood 1913) (8C, O). *Demirastrites triangulatus* disappeared in the lower part of the *pectinatus* Biozone along with *P. concinnus* (Fig. 8Q). Early species of *Campograptus* were joined by *Campograptus pseudoplanus* (Sudbury 1958). Uncommon specimens of '*M.*' *walkerae rheidolensis* (Fig. 8I) continued to the upper part of the biozone. Monograptids of the genus *Pernerograptus* are represented by *P. sudburiae* and the less common *P. chrysalis* (Zalasiewicz 1992) (Fig. 8B). Specimens of *Pribylograptus* sp. with long ventral apertural spines closely resemble a species figured by Loydell *et al.* (2003, fig. 4q) as *Pribylograptus* sp. from the *triangulatus* Biozone of Latvia. *Rhaphidograptus toernquisti* (Fig. 8G) dominated among biserial taxa, being accompanied by less abundant specimens of *M. undulatus*, *G. perneri*, *Normalograptus scalaris* (Hisinger 1837) (Fig. 8E), *Rickardsograptus thuringiacus* (Kirste 1919) (Fig. 8L), *Petalolithus minor* (Elles 1897) (Fig. 8H), *P. ovatoelongatus* (Fig. 8J), and the earliest specimens of *Petalolithus praecursor* Bouček & Přibyl 1942. *Neodiplograptus magnus*, *P. inopinatus* (Fig. 8A) and *P. finneyi* have their highest occurrences in the lower and/or middle part of the *pectinatus* Biozone, the total graptolite fauna of which comprises 30 species.

Black shales are gradually replaced by siliceous strata in the upper part of the *pectinatus* Biozone, including silty silicites, which alternate with siliceous shales through the succeeding 1-m-thick *Demirastrites simulans* Biozone. *Demirastrites simulans* (Pedersen 1922) and *Pseudorthograptus insectiformis* (Nicholson 1869), along with several taxa continuing

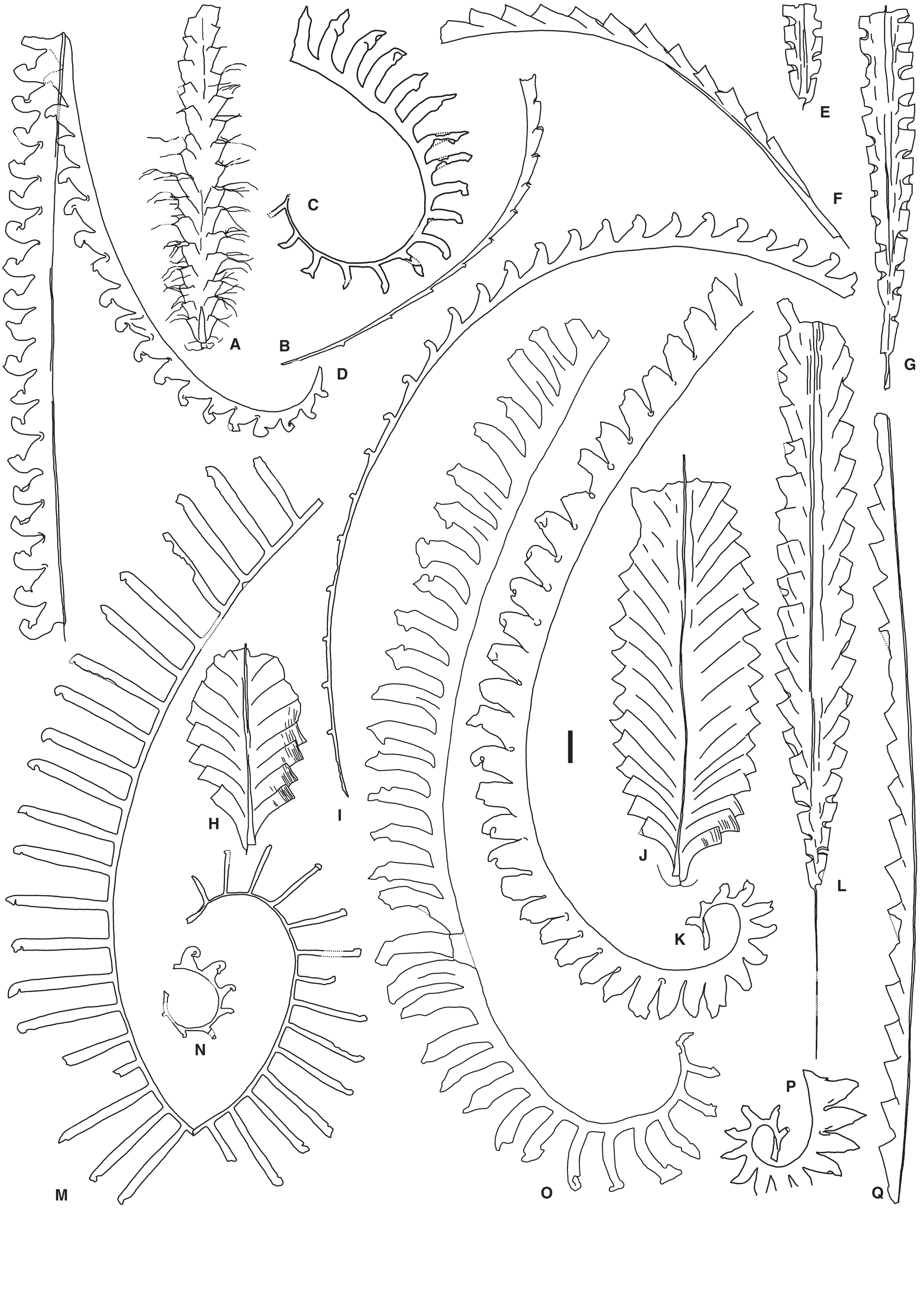
A
B
C
D
E
F
G
H
I
J
K
L
M
N
O
P
Q

Fig. 8. Graptolite fauna of the lower Aeronian *Demirastrites pectinatus* Biozone – selected taxa. A, *Pseudorthograptus inopinatus* (Bouček 1944), PŠ 4011, sample HT120–130. B. *Pernerograptus*? *chrysalis* (Zalasiewicz 1992), PŠ 4020, mesial part from sample HT120–130. C, O, *Demirastrites major* (Elles & Wood 1913). C, PŠ 3925, sample HT90–100. O, PŠ 3929, sample HT90–100. D, *Campograptus communis* (Lapworth 1876), PŠ 3960, broken rhabdosome from sample HT120–130. E, *Normalograptus scalaris* (Hisinger 1837), PŠ 4102, juvenile rhabdosome from sample HT40–50. F, *Coronograptus gregarius* (Lapworth 1876), PŠ 3918, late form with long sicula from sample HT90–100. G, *Rhaphidograptus toernquisti* (Elles & Wood 1906), PŠ 4106/2, sample HT30–40. H, *Petalolithus minor* (Elles 1897), PŠ 3951, sample HT70–80. I, '*Monograptus*' *walkerae rheidolensis* Rickards *et al.* 1977, PŠ 4009, sample HT100–110. J, *Petalolithus ovatoelongatus* (Kurck 1882), PŠ 4018, sample HT90–100. K, P, *Demirastrites pectinatus* (Richter 1853). K, PŠ 4057, sample HT70–80. P, PŠ 3931, sample HT90–100. L, *Rickardsograptus thuringiacus* (Kirste 1919), PŠ 4100, sample HT10–20. M, *Rastrites longispinus* Perner 1897, PŠ 4015, broken mature rhabdosome from sample HT110–120. N, *Torquigraptus* sp. aff. *denticulatus* (Törnquist 1899), PŠ 4068a, juvenile specimen from sample HT70–80. Q, *Pristiograptus concinnus* (Lapworth 1876), PŠ 4125, mesial fragment from sample HT130–140. All specimens from the Hlásná Třebaň Section, scale bar represents 1 mm.

from the *pectinatus* Biozone, including *D. pectinatus*, *R. longispinus* and *R. toernquisti*, have their last appearance in the lower part of the biozone. The full list of graptolites and their stratigraphical ranges from the upper *vesiculosus* to the lower *simulans* biozones are shown in Figure 4.

Higher in the succession, beyond the interval presented on Figure 4, *Rastrites geinitzii* Törnquist 1907; *Monograptus mirus* Perner 1897 and *Campograptus millepeda* (M'Coy 1850) joined the assemblage of the *simulans* Biozone in the Hlásná Třebaň section.

Black siliceous shales interbedded with platy, black silty silicites characterize the 1.3-m-thick *Pribylograptus leptotheca* Biozone and the more than 2 m thickness of the lower half of *Lituigraptus convolutus* Biozone. These higher strata were thermally influenced by an overlying ca. 2-m-thick basalt sill, which intruded into the overlying black shales and pale-coloured mudstones of the lower Lithohlavy Formation. Graptolites are less well-preserved and difficult to collect from the thermally altered silicites, but the general faunal composition matches that described by Štorch (1998) from Tmaň.

Forty-two samples of black shales were taken at 10 cm intervals and processed for organic-walled microfossils. Thinner, 5-cm-thick intervals were sampled from the immediate Rhuddanian–Aeronian boundary strata. Preliminary data by Butcher (2016) complement the largely Rhuddanian chitinozoan data published by Dufka & Fatka (1993) and extend the results into the Aeronian. Preliminary results (A. Butcher, personal communication, 2016) suggest that the boundary interval occurs within *maennili* chitinozoan Biozone, which is consistent with data from the type Llandovery area (Davies *et al.* 2013).

Sedimentary succession

Three principal hemipelagic lithotypes (Fig. 9) are developed in the lower Silurian Želkovice Formation in the Hlásná Třebaň section. The stratigraphical distribution of the three lithotypes is consistent with other sections of the southern limb of the Prague Synform (see Fig. 2).

Black silty-micaceous laminites. – This lithotype comprises claystones densely intercalated with medium to poorly sorted silt laminae, which are generally about 0.5 mm thick and mainly composed of subangular grains of quartz and K-feldspar (with an albite component) (Fig. 9A). To a lesser extent, muscovite laths and framboidal pyrite, the latter replacing organic matter remnants, occur in the silt laminae. Well-rounded zircon grains are rare. In the claystone intercalations, discontinuous, ca. 40-μm-thick laminae composed exclusively of organic matter are common and could possibly represent either microbial mats or other compacted organic material. Moreover, skeletal TiO_2 (rutile – ?ilmenite alteration product suggesting *in situ* crystallization) is a common feature of the clay matrix.

The thickness of the interval of laminites is about 70 cm, starting at the lower disconformity, that is also documented by the gap in graptolite record (see Fig. 4). The second disconformity is developed about 30 cm above the base of the laminites, and above this the laminites fine upward. The transition between the laminites and black shales is gradational and occurs within an interval about 100 cm in thickness in which sets of silty-micaceous laminae alternate with black shale. Laminites with high TOC (ca. 6 wt. %) and lacking any benthic body fossils or trace fossils suggest deposition in an anoxic or euxinic environment. In the *acuminatus* Biozone, however, two thin beds of pale mudstone intercalated within the laminite succession can be interpreted to indicate a temporary increase of clastic material input and, perhaps, disruption of anoxic conditions. These laminites have been interpreted by Oczlon (1992) as deposits from contour currents sweeping a high region of the sea bottom. This interpretation is supported by the palaeogeographic distribution of laminites in the Prague Synform and their association with gaps in the sedimentary logs as described above (Štorch 2006).

Black shales. – Black shales were deposited in the Hlasná Třebaň section from the upper *cyphus* Biozone, through the Rhuddanian–Aeronian boundary, to the lower *pectinatus* Biozone (Fig. 9B). This

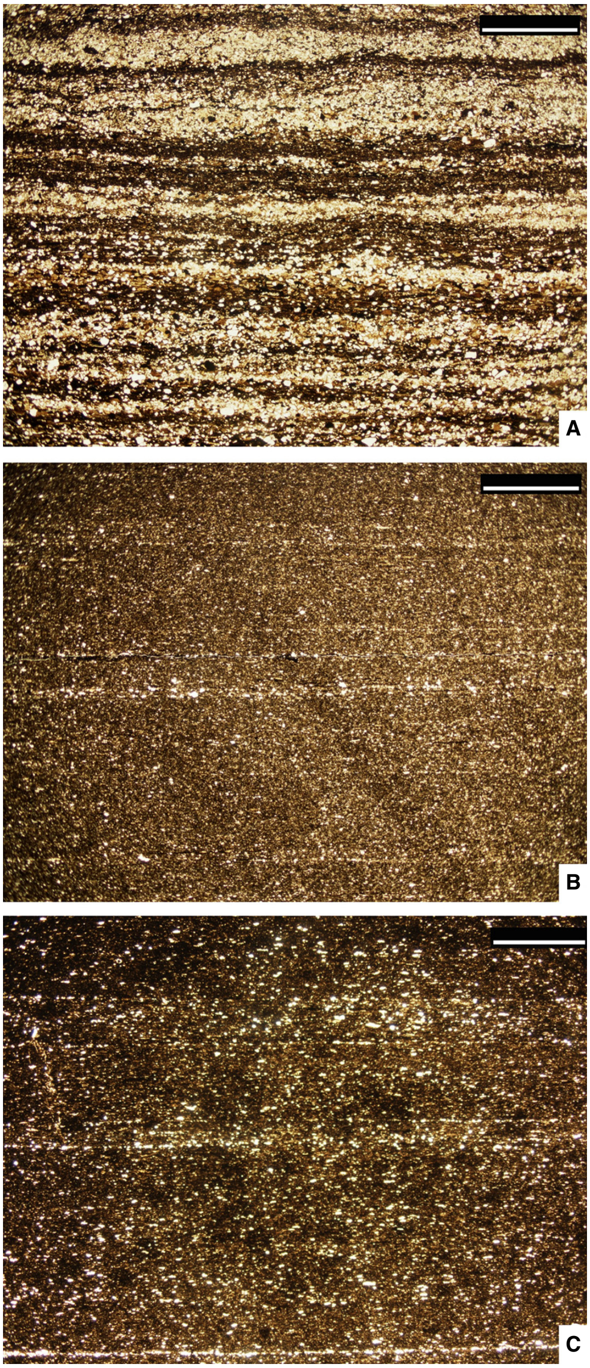

Fig. 9. Thin sections of principal lithotypes developed in the Rhuddanian–Aeronian succession at Hlásná Třebaň. A, silty-micaceous laminite, *acuminatus* Biozone. B, black shale, uppermost *cyphus* Biozone. C, black siliceous shale, *pectinatus* Biozone. Scale bar represents 2 mm.

lithotype consists of laminated claystones (grain size < 20 μm) with dispersed grains of quartz, K-feldspar and muscovite of a maximum grain size of 40 μm. Discontinuous laminae of organic matter with dispersed pyrite up to 5 μm thick are common. In addition, two discontinuously zoned, *in situ* crystallized barium K-feldspar grains were found, which could point to low temperature fluid alteration of the claystones. The lower Silurian graptolitic black shales that are spread across peri-Gondwanan Europe are widely regarded as offshore anoxic deposits. Poorly developed lamination in these strata at Hlásná Třebaň may be the result of relatively continuous hemipelagic sedimentation without significant breaks or variations.

Black siliceous and silty shales (silty silicites, Fig. 9C). – Shales developed gradationally from the previous lithotype in the upper part of studied log. This facies consists of couplets of about 5-cm-thick intervals of siliceous shale and about 10-cm-thick silty, coarsely laminated shale enriched in silica (silty silicite). The transition between both lithologies is gradual on a scale of a few millimetres. Exceptional K-feldspar and muscovite grains up to a maximum size of 50 μm are dispersed in the laminated shale matrix with abundant, mainly quartz grains <20 μm. Partially recrystallized quartz grains form silica cement. Discontinuous, 15-μm-thick laminae composed entirely of organic matter are common. Phosphates occur within this lithofacies, characterized by crandallite and churchite grains, and the latter are enveloped by organic matter. The origin of remobilized silica remains unclear as primary sedimentary textures were obscured by diagenetic processes, although it appears to be linked with either recurrent periods of increased input of fine-grained clastic quartz or primary cyclicity due to periodic enrichment of the sediment by biogenic silica, although no undoubted radiolarians or sponges were found.

Whole-rock geochemistry

Detrital-input element proxies. – The PAAS-normalized multi-element plot (Fig. 10; Taylor & McLennan 1985) for the Hlásná Třebaň samples illustrates a distinct depletion of most elements in most samples compared to PAAS, with the exception of the pronounced positive anomalies of Ba, U and Ce. Moreover, for the Rhuddanian samples, Nb and Ti are also elevated, probably due to increased occurrence of zircon, biotite and TiO_2 (?rutile) in the Rhuddanian sandy-micaceous laminites. In contrast, the Aeronian samples, particularly those from the *pectinatus* Biozone, yielded the highest P concentrations, which possibly reflect the presence of common phosphates (crandallite and churchite) in the siliceous shale facies. A prominent peak in Hf and Zr corresponds to the pale mudstone from the *acuminatus* Biozone and could be linked to an increased

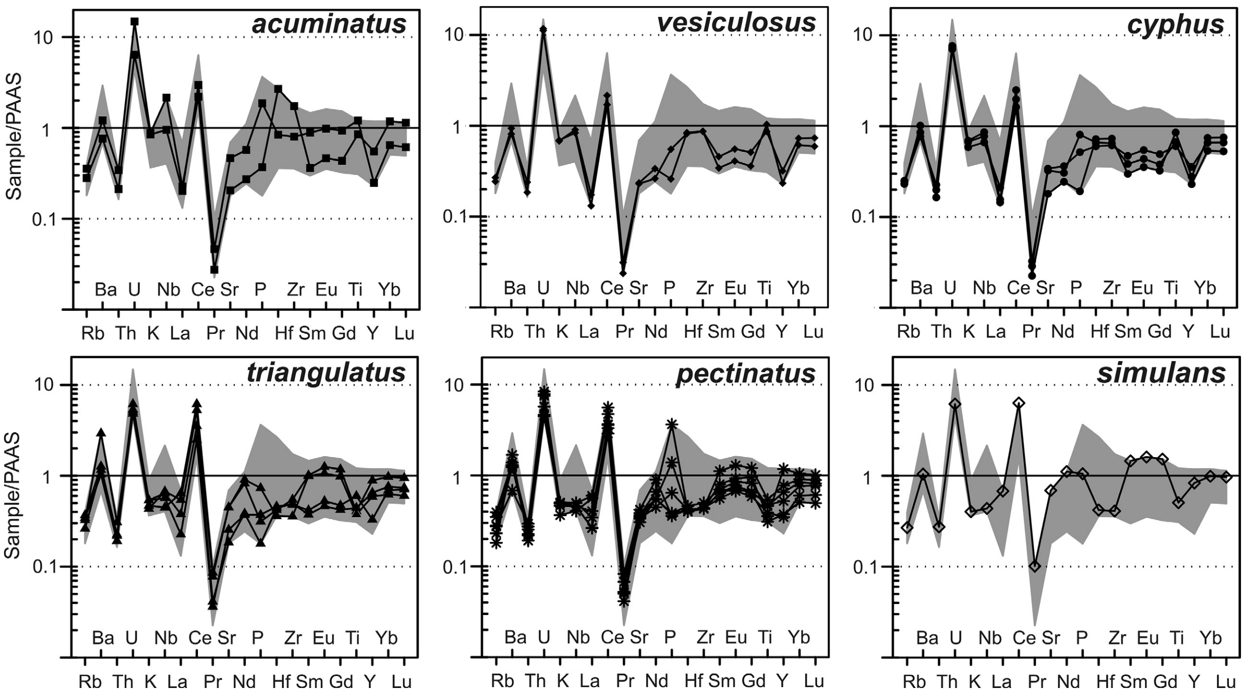

Fig. 10. PAAS-normalized (Taylor & McLennan 1985) spiderplots of the Hlásná Třebaň samples. The grey field portrays the overall variability in the whole data set.

concentration of zircon grains compared to the rest of shales. Elevated Ba contents suggest that some fluid alteration may have been involved, which is further supported by occurrence of barium feldspars. Spiderplot patterns of the Hlásná Třebaň samples (Fig. 10) lack any significant Eu anomaly (Eu/Eu* = 1.1–1.2), which rules out any significant diagenetic effects or hydrothermal fluid influence on shale geochemical composition (Sverjensky 1984; MacRae *et al.* 1992). However, the Ce anomaly (Ce/Ce* = 0.9–1.1; see Fig. 10 and *'Redox element proxies'*, below) truly reflects redox reactions – possible anomalous abundances of La can be ruled out as the Pr/Pr* ratios are in the range of 0.2 to 0.3 (Bau & Dulski 1996).

In addition, the Hlásná Třebaň PAAS-normalized patterns (Fig. 10) represent more REE-depleted compositions when compared to Ordovician, Cambrian or even certain Neoproterozoic sediments (Drost 2008), which could point to the increased contribution of a 'primitive' basic volcanic component to the clastic material in the Rhuddanian and Aeronian sediments.

Changes in concentrations of terrigenous elements (e.g. Al and Ti) are used for evaluation of siliclastic material supply as the Ti/Al declines gradually as a result of heavy mineral fractionation during transport (Calvert & Pedersen 2007). The Ti/Al in Hlásná Třebaň samples (Fig. 11) gradually decreased through the Rhuddanian to basal Aeronian, lacking significant fluctuations through the rest of the studied interval. Three maxima – at the base of the *acuminatus*, middle of the *vesiculosus* and in the upper *cyphus* biozones – are preserved in the micaceous laminite facies and probably reflect higher heavy mineral content in coarser, silty laminae. Compared to the Aeronian (Ti/Al = 0.08–0.12), however, the higher Ti/Al ratios (0.13–0.23) in the Rhuddanian strata could either represent a fluctuation in siliciclastic input, such as heavy fraction concentration in silty laminae (possibly due to contourite or turbidite current washout) or could simply reflect closer proximity to the source area.

Variations in La/Th, rather pronounced in the Aeronian strata (La/Th = 2.6–7.6) but more-or-less constant in the Rhuddanian samples (La/Th = 1.7–3.3), could also provide a clue to sedimentary source character. According to Floyd & Leveridge (1987), these La/Th values (~ 2–8) could reflect derivation from upper continental crust combined with a mixed felsic/basic source. Moreover, low La/Sc (0.5–3.4) and high Ti/Zr (14–43) suggest an island arc setting (Bhatia & Crook 1986), which correlates with the geochemical character of the Neoproterozoic basement (Drost 2008).

Redox element proxies. – Cerium concentrations can reflect redox conditions of the overlying water column and are resistant to changes during burial and diagenesis (Wignall 1994). Calculated Ce/Ce*

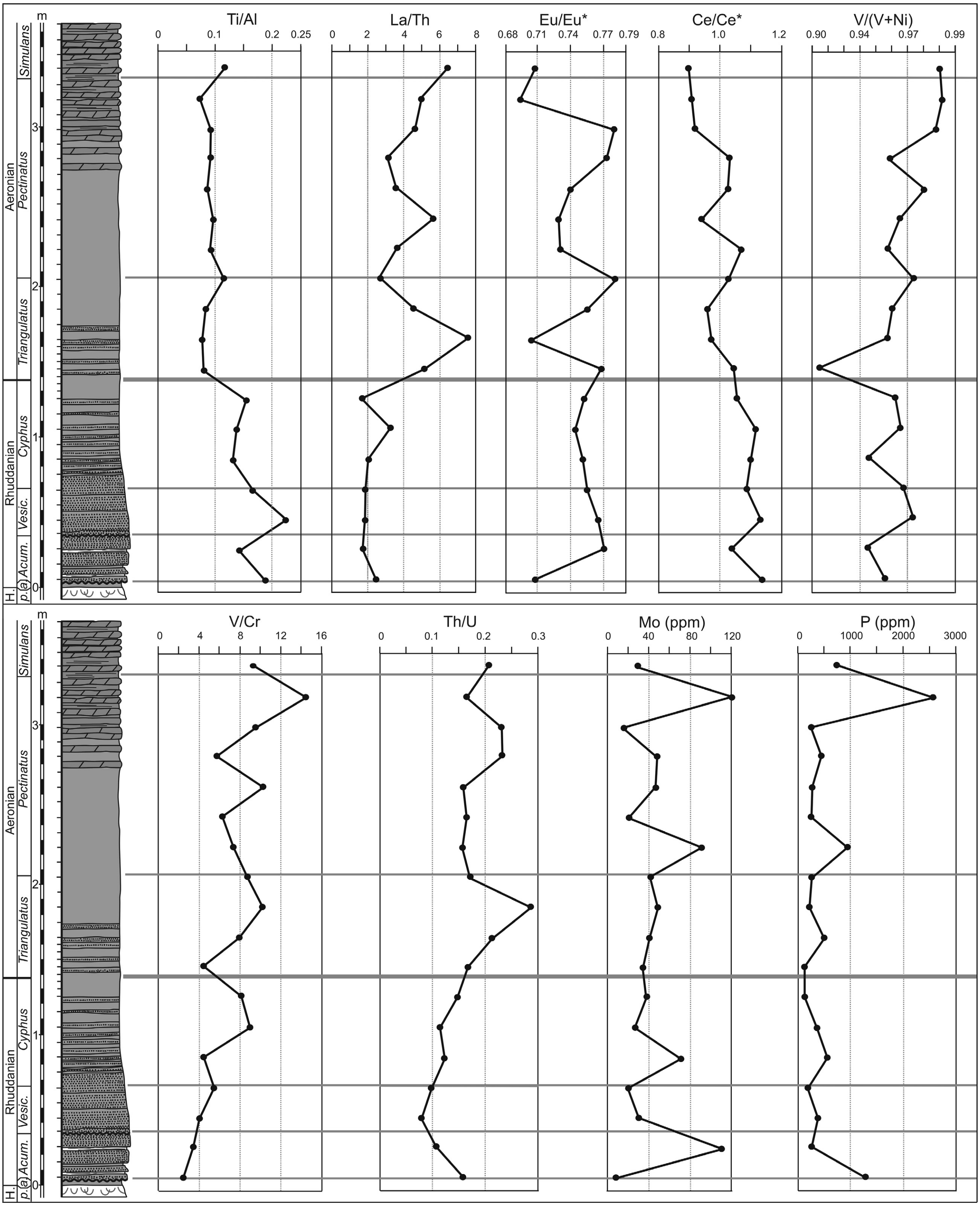

Fig. 11. Stratigraphical distribution and values of selected ratios of sedimentary proxies and redox-sensitive trace elements. See Figure 4 for lithology explanations and abbreviations.

values of the Hlásná Třebaň samples yielded variations from 0.90 to 1.14 (Fig. 11). Possible correlation of positive Ce/Ce* values with zircon accumulations in shales can be ruled out with the exception of the pale mudstone from the *acuminatus* Biozone (Fig. 11), which reached the highest

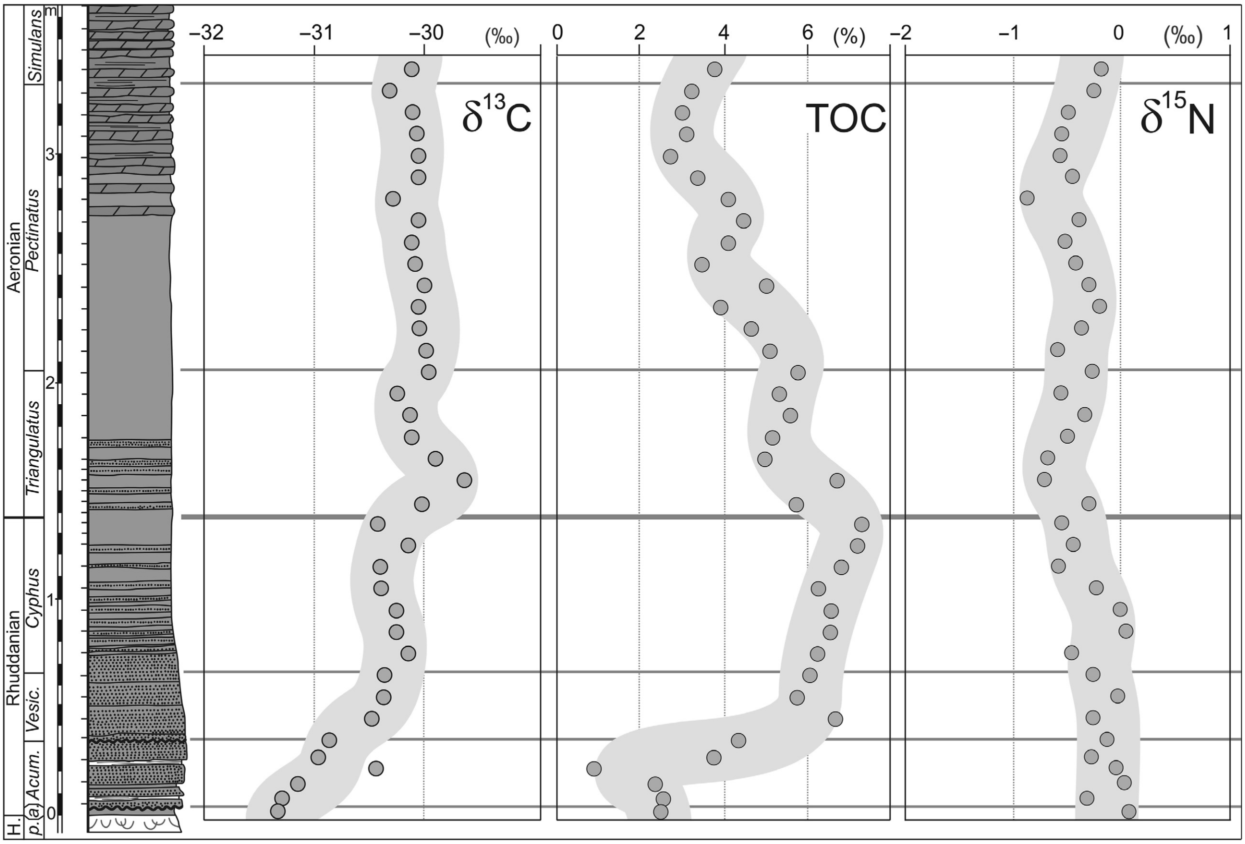

Fig. 12. C_{org} and N_{bulk} isotopic record in the Hlasná Třebaň section plotted with TOC. See Figure 4 for lithology explanations and abbreviations.

positive Ce/Ce* (1.14) values and the highest Zr content (364 ppm). Excluding that sample, Ce/Ce* ratios of 1.04–1.14 suggest that the Rhuddanian sediments were deposited under anoxic (reducing) conditions. On the other hand, certain intervals of the Aeronian (middle of the *triangulatus* and upper *pectinatus* biozones) could have been deposited under anoxic conditions interrupted by occasional bottom ventilation, based on the evidence of the record (Ce/Ce* = 0.90–1.07).

Vanadium is a redox-sensitive element, the sedimentary geochemistry of which is similar to that of Ni, although subtle variations in their ratios are capable of providing useful palaeoenvironmental information (Wignall 1994). In particular, V/(V+Ni) can serve as a redox proxy (Fig. 11). Wignall (1994) suggested that V/(V+Ni) ratios of 1–0.83 are indicative of euxinic conditions, 0.83–0.57 for anoxic conditions, 0.57–0.46 for dysoxic conditions and <0.46 for oxic conditions. In the Hlásná Třebaň samples, both V and Ni seem to be authigenic based on comparison with the detrital-input proxies, Ti/Al and Zr (Fig. 11), although it cannot be ruled out that the V/(V+Ni) values in the laminites of the *acuminatus* and *vesiculosus* biozones could be obscured by detrital input of vanadium, shifting the V/(V+Ni) proxies to higher (more typically euxinic) levels (Fig. 11). Taking into account V/(V+Ni) values ranging from 0.90 to 0.98, the sedimentary record of the Hlásná Třebaň section could have reflected deposition under euxinic conditions, which is supported by the abundant occurrence of framboidal pyrites in the laminite facies. However, the size of the pyrite framboids ranges from 5 to 10 μm in diameter, which correlates with a syngenetic origin (<6 μm), that is within euxinic water column, but with a diagenetic origin (>6 μm), that is within sediment (Wilkin *et al.* 1996; Wignall *et al.* 2005). A possible explanation of the occurrence of both syngenetic and diagenetic pyrite occurrence could be intermittent euxinia.

A minimum V/(V+Ni) value of 0.90, possibly representing a shift towards more anoxic (rather than euxinic) conditions, is recorded at the base of the *triangulatus* Biozone, that is at the base of Aeronian (Fig. 11). The redox character of the depositional conditions can also be interpreted from the V/Cr index (Jones & Manning 1994) (Fig. 11). Ratios of V/Cr are in the range of 2.5–3.4 in the *acuminatus* Biozone, 4.1–5.5 in the *vesiculosus* Biozone, 4.4–9.0

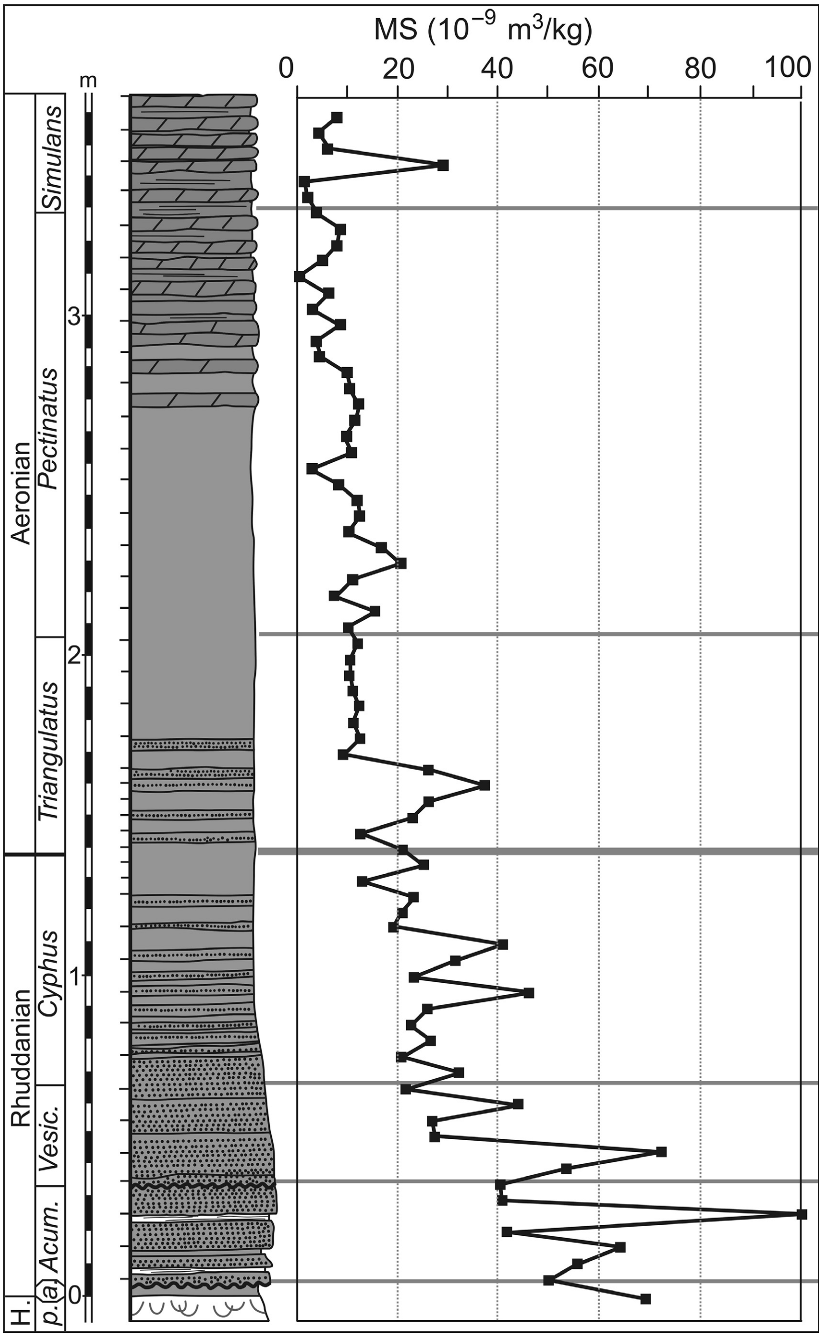

Fig. 13. Magnetic susceptibility in the Hlasná Třebaň section. See Figure 4 for lithology explanations and abbreviations.

in the *cyphus* Biozone, 4.4–10.3 in the *triangulatus* Biozone, 5.6–14.4 in the *pectinatus* Biozone and 9.27 in the *simulans* Biozone. This evidence appears to suggest dysoxic–anoxic conditions for the *acuminatus*–*vesiculosus* biozones and anoxic conditions during deposition of the *cyphus*–*simulans* biozones. However, Cr positively correlates with Ti/Al and Zr proxies, and hence, its concentration may not be authigenic but rather dependent on detrital input, which may have caused the apparent shift towards dysoxic values (2.5–4.1 of V/Cr) in the *acuminatus* and *vesiculosus* biozones as well as possibly lowered the values indicating anoxia in the rest of the succession.

The Th/U ratio can also serve as a proxy for the redox conditions of a depositional environment, distinguishing anoxia at values of Th/U < 2 (Wignall 1994; Wignall & Twitchett 1996). The black-shale succession of the Hlásná Třebaň section yielded low Th/U values in the range of 0.08–0.29 (Fig. 11), which is typical for anoxic environments. The values of Th/U gradually increase from the *vesiculosus* Biozone to the upper *triangulatus* Biozone, with a marked drop at the base of *pectinatus* Biozone. The upper part of the *pectinatus* Biozone, characterized by the onset of siliceous shales, possibly reflected a shift towards less reducing depositional conditions, but still anoxic, as documented by an increase in Th/U, and a decrease in V/(V+Ni) and V/Cr. The *acuminatus* Biozone is marked by decreasing Th/U and V/(V+Ni) values and by an increase in V/Cr, which could possibly correspond to a lower detrital component, related to the lower frequency of coarse silty laminae.

Molybdenum contents (8–122 ppm) do not correlate either with V/(V+Ni) (Fig. 11) or with TOC (Fig. 12) in the *acuminatus–triangulatus* biozones. However, the highest Mo contents in shales of the *pectinatus* Biozone fit slightly better with the V/(V+Ni), and also with the TOC curve. The latter could be explained by additional release and reduction in molybdenum from organic matter, and this would point to the presence of anoxic pore waters (Calvert & Pedersen 1993). However, the lack of correlation of Mo with TOC in the Rhuddanian shales and laminites and also samples from Aeronian *triangulatus* Biozone indicates Mo uptake from water by authigenic sulphides, which commonly form in anoxic conditions, generally most rapidly under euxinic conditions (Algeo & Maynard 2004). In addition, phosphorus contents (125–2546 ppm), serving as palaeoproductivity proxy, show a similar pattern to those of molybdenum (Fig. 11). Therefore, shales of the *pectinatus* Biozone appear to have preserved remineralized P, which was not released into the water column during decomposition of organic matter but remained immobilized in phosphatic form in the shales. On the other hand, phosphorus released by organic decomposition from the *acuminatus–triangulatus* biozones was likely lost into water column.

In summary, the body of evidence from geochemical redox proxies; that is, Ce/Ce*, V/(V+Ni), Th/U and Mo suggest that the black shales of the Hlásná Třebaň section were deposited under anoxic or even euxinic conditions. Euxinia is documented by presence of framboidal pyrite (<6 μm in diameter) in shales within the *acuminatus* Biozone and values of V/(V+Ni) of the samples from *acuminatus* and *vesiculosus* biozones. The base of the *triangulatus* Biozone (base of Aeronian) is marked by evidence, primarily in V/(V+Ni), V/Cr, Th/U and to lesser extent in Ce/Ce*, of a change to less reducing (anoxic, rather than euxinic) depositional conditions. However, it must be noted that values of V/Cr reflect detrital input rather than depositional conditions.

TOC and organic carbon and nitrogen isotope geochemistry

Newly gathered data on TOC and organic carbon isotope compositions (Fig. 12) have confirmed the previously published data (Frýda & Štorch 2014), collected from another outcrop at Hlasná Třebaň, situated about 8 metres SW of the present section in its lower part (Fig. 3). Note that Frýda & Štorch (2014) did not recognize the presence of the upper paraconformity or the occurrence of the *acuminatus* Biozone in lower part of their section, following the biostratigraphical data of Štorch (2006). Therefore, a thin stratigraphical interval between the lower and upper paraconformities (i.e. samples HT–323, HT–330 and HT–340; see Fig. 4) belonging to the *acuminatus* Biozone is identical with the lithological sequence from about 5 to 40 cm above the Ordovician–Silurian boundary shown by Frýda & Štorch (2014, fig. 4) and presented in that paper as the lower part of their *vesiculosus* Biozone.

The $\delta^{15}N_{bulk}$ values vary from −0.9 to 0.1‰ across the measured section and revealed a weak, but statistically significant decreasing trend from the *cyphus* to the middle of *triangulatus* Biozone, from which point the $\delta^{15}N_{bulk}$ values start to increase upward to the lower part of the *pectinatus* Biozone (Fig. 12). The $\delta^{15}N_{bulk}$ values in the remaining part of the *pectinatus* Biozone seem to slightly, but significantly decrease and again increase in the youngest strata (Fig. 12).

The Rhuddanian–Aeronian boundary interval exhibits no important change in the evolution of the nitrogen isotopic record and may be characterized by $\delta^{15}N_{bulk}$ values of about −0.5‰. On the other hand, the organic carbon isotope record exhibits a minor positive excursion just above the base of the *triangulatus* Biozone. The TOC content increases from the *vesiculosus* Biozone upwards and reaches its highest values close to the Rhuddanian–Aeronian boundary from which level it significantly decreases upwards (Fig. 12).

Probably not all short-term $\delta^{13}C_{org}$ and $\delta^{15}N_{bulk}$ fluctuations can be recognized because of the rather low rate of sedimentation at the Hlásná Třebaň section. Nevertheless, the $\delta^{15}N_{bulk}$ data suggest that the community of primary producers did not significantly change through the studied interval. Although the identity of the primary producers is difficult to determine without additional data on organic chemistry (e.g. Capone *et al.* 2008), the values recorded in this succession are similar to those reported from the lower Rhuddanian strata in Arctic Canada (Melchin *et al.* 2013) and South China (Luo *et al.* 2016). In those studies the similar, slightly negative $\delta^{15}N$

values were interpreted to represent conditions of intense denitrification taking place in anoxic deep waters, resulting in bacterial fixation as the principal source of biologically available N in surface waters. This interpretation (i.e. the presence of anoxic deep waters) is consistent with the geochemical redox proxy data presented here, as well as the lithofacies and faunal data, which indicate anoxic to euxinic conditions through the studied interval.

On the other hand, the TOC record revealed a distinct change at the level proposed herein to mark the base of the Aeronian Stage of the Silurian System. Rather constant TOC values of about 6 wt. % in the upper part of the Rhuddanian succession start to decrease significantly. It is difficult to determine whether the decreasing trend was caused by an increasing rate of sedimentation or by a decreasing of palaeoproductivity.

Our new $\delta^{13}C_{org}$ data have confirmed the results of the previous study of this locality by Frýda & Štorch (2014). Our data show a minor but statistically significant positive excursion just above the base of the *triangulatus* Biozone (Fig. 12). Despite its relatively small magnitude, this positive $\delta^{13}C_{org}$ excursion may have considerable significance for global correlation of the interval near the GSSP (see further discussion below).

Magnetic susceptibility

Magnetic susceptibility (MS) data show a prominent decreasing trend (from values around 70 to around $20 \times 10^{-9} m^3/kg$) and an oscillatory pattern in the lower and middle Rhuddanian succession beginning from the incomplete *ascensus, acuminatus* and *vesiculosus* biozones, through the *cyphus* Biozone towards the base of the Aeronian (Fig. 13). In the lower part of the Aeronian succession, in the *triangulatus* and *pectinatus* zones, MS data show quite low and uniform values without significant peaks or variations (average value $10.5 \times 10^{-9} m^3/kg$), except at around the 185 cm level. The general decreasing trend continues towards the base of the *simulans* Biozone. The MS curve through the studied section strongly reflects the changing lithology. Oscillations in the MS values in the lower and middle part of the Rhuddanian succession, represented by the silty-micaceous laminites in the lowermost part of the studied section and alternating with black shales higher in the section, reflect the decreasing proportion of coarser detrital material and probably also a change in the mineralogy (a slightly increased amount of dispersed limonite). In the upper half of the *triangulatus* and lower half of the *pectinatus* biozones MS oscillations disappear, which reflects the prevailing uniform lithology of black shale with almost no silty-micaceous intercalations or laminae. A further decrease in MS values in the upper part of the *pectinatus* Biozone and lowermost part of the *simulans* Biozone reflects an increasing proportion of a diamagnetic component – quartz – in the black shales and a lithology that is changing towards siliceous shales and silty silicites.

Suitability of the Hlásná Třebaň section as a stratotype section

The section proposed as the GSSP, located near the village of Hlásná Třebaň, fulfils all of the requirements for boundary stratotype listed by Cowie *et al.* (1986) and Salvador (1994). Sedimentation within the boundary interval, although somewhat condensed, shows no evidence of a break or facies change based on faunal, lithological or geochemical criteria. An abundant and diverse graptolite fauna is present in all of the Aeronian and Rhuddanian strata. Identifiable chitinozoans are also known to occur, are currently under detailed study and have already been used to identify the biozonation through the boundary interval. There are no significant structural complexities. The stratigraphical succession, comprising the upper Hirnantian, Rhuddanian and lower and middle Aeronian (*ascensus – convolutus* biozones), is well exposed on a hillslope. The succession has also produced a useful isotope record with a recognizable carbon isotope excursion near the boundary level. The section lies within the Bohemian Karst protected landscape area, and both study and access by a narrow footpath uphill from the road from Hlásná Třebaň to Rovina are unrestricted. Hlásná Třebaň is readily accessible by car and train from Prague in a half an hour. In addition, the succession lies within the historically important Barrandian area, which has been a classic reference area for our understanding the Silurian System for over 100 years.

Graptolite fauna across the Rhuddanian–Aeronian boundary – biodiversity and palaeobiogeography

In the Prague Synform, the uppermost Rhuddanian and lowermost Aeronian beds yield a highly diverse graptolite fauna, which represents a substantial part of global graptolite species diversity. Global diversity reached a maximum of slightly over 60 species in the early Aeronian according to Cooper *et al.* (2014). Of this number, 31 species have been found in the *triangulatus* Biozone of the Hlásná Třebaň section itself.

Among biserial graptolites, the long-ranging *R. toernquisti* predominates through the boundary interval, being accompanied by *Metaclimacograptus* aff. *slalom* and abundant specimens of *M. undulatus*. Glyptograptids of *G. tamariscus* affinity are difficult to identify to the species and subspecies level when unfavourably preserved, so we have grouped these forms as *Glyptograptus* ex gr. *tamariscus*. *Glyptograptus perneri* made its lowest occurrence 3 cm below the FAD of *D. triangulatus* in the Hlásná Třebaň section. The Rhuddanian–Aeronian boundary interval is further characterized by the incoming of the relatively common and easily identified *P. finneyi* (FAD ca. 10 cm below FAD of *D. triangulatus*) and *P. inopinatus* (FAD ca. 3 cm below the FAD of *D. triangulatus*), both of which range through the *triangulatus* Biozone to the lower part of the *pectinatus* Biozone (Fig. 4). *Pseudorthograptus inopinatus* is known from the *triangulatus* Biozone of northeastern Spain (Gutierrez-Marco & Štorch 1998) and Morocco (Willefert 1963) and probably the *cyphus* Biozone of the south Urals in Kazakhstan and the Arctic Canada (Koren' & Rickards 1996). Unpublished information from Arctic Canada suggests that *P. inopinatus* makes its first appearance in the uppermost part of the *cyphus* or lower *triangulatus* Biozone and extends through much of the early Aeronian (Russel-Houston 2001). *Pseudorthograptus finneyi* is recorded to date solely from the Hlinsko area of NE Bohemia (Štorch & Kraft 2009) and the Prague Synform of Central Bohemia, although it has very recently been found to occur also in Wales at the same stratigraphical level (M.J. Melchin personal observation, 2015). In addition, some of the earlier European records of *Rivagraptus cyperoides* (Törnquist 1897) may, in fact, represent specimens of *P. finneyi*, as was the case in Bohemia (Bouček 1953; Štorch 1994). *Pseudorthograptus mitchelli* disappeared in the uppermost part of the *cyphus* Biozone but *P. obuti*, which occurs from the Urals through Lithuania, Norway, Thuringia, and Bohemia (see Štorch 2015 for discussion) to Morocco (P. Štorch personal observation, 2016), survived into the lowermost *triangulatus* Biozone (e.g. ca. 8 cm above the base in Hlásná Třebaň), where it is replaced by *P. ovatoelongatus*. The latter species is the earliest known representative of the genus *Petalolithus* and is a relatively cosmopolitan form, occurring across peri-Gondwana, Avalonia and Baltica. It has also been reported in some circum-equatorial regions (*sensu* Melchin 1989), such as the Gorny Altai (Sennikov 1976; Sennikov *et al.* 2008) and Norilsk (Obut *et al.* 1968) regions of Siberia.

The stratigraphically highest specimens of *Neodiplograptus fezzanensis*, which are rarely found in the *triangulatus* Biozone, occur just below the FAD of the closely similar species, *Neodiplograptus magnus*, in the middle part of the *triangulatus* Biozone. *Neodiplograptus fezzanensis* represents a typical element of the Gondwanan and peri-Gondwanan realm (Algeria, Bohemia, Libya, Morocco, Niger, Spain; Štorch & Massa 2003) in the *cyphus* Biozone, whereas *N. magnus* is an abundant zonal index-species in the Welsh Basin and other parts of Great Britain (Toghill 1968; Zalasiewicz & Tunnicliff 1994; Zalasiewicz *et al.* 2009). In Great Britain, however, the lowest occurrence of *N. magnus* is much higher than in the Prague Synform, above the FAD of *Demirastrites fimbriatus* (Nicholson 1868a), which is a junior synonym of *Demirastrites pectinatus* (Richter 1853) as recognized in this paper.

Monograptid graptolites underwent remarkable diversification in both number of taxa and variety of morphologies in the Rhuddanian–Aeronian boundary interval. The almost simultaneous appearance of several genera with novel isolated and hooked triangular thecae (Fig. 7D, G, H, J, L–N, P: *Demirastrites, Rastrites, Campograptus*) has a good potential for global biostratigraphical correlation despite the fact that relatively few of the individual species have been shown to be truly cosmopolitan. In the Prague Synform and the Hlásná Třebaň section itself, for example, the base of the Aeronian succession is marked by the FAD of *D. triangulatus*, the earliest known species with isolated high-triangular thecae furnished with laterally extended apertural hooks. This species is widely distributed in peri-Gondwana, Avalonia and Baltica, but the morphology of specimens previously assigned to this species in the circum-equatorial province of Melchin (1989), comprising North America, Siberia and China, shows some morphological differences from the typical European material. In some instances, these specimens likely belong to different species, but in some other cases, the differences may be the result of geographical, intraspecific variation. The taxonomic work that is needed to clarify the taxonomy and palaeogeographical distribution of some of these forms is currently under way.

The uppermost Rhuddanian strata at Hlásná Třebaň can be distinguished by abundant and easily recognizable rhabdosomes of the zonal index-species, *C. cyphus*, associated with early populations of *C. gregarius*, abundant specimens of *P. sudburiae* [formerly assigned to *Monograptus argutus* (Lapworth 1876) by Bouček 1953 and Štorch 1994], as well as the commonly occurring *P. difformis*. *Coronograptus cyphus* disappears 1–2 cm below the lowest occurrence of *D. triangulatus*, whereas the LAD of *P. difformis* is ca. 3 cm above. In addition, *P. revolutus* is confined to the boundary interval. *Pernerograptus* sp. nov. (Fig. 5K), readily distinguished by its crook-shaped rhabdosome with few triangular mesial thecae and a rather short proximal part, was detected 1–3 cm below the boundary. This form is a distinctive element of the graptolite assemblage of the uppermost *cyphus* Biozone in Spanish sections (P. Štorch personal observation, 2014). Rhabdosomes questionably assigned to *P. sequens* have been recorded in several samples of the *triangulatus* Biozone, beginning 2 cm above the base of the Rhuddanian succession. This species, apparently confined to middle part of the *triangulatus* Biozone in Wales (Zalasiewicz *et al.* 2009), was also reported by Bjerreskov (1975) from upper *triangulatus* and lower *pectinatus* subzones of *Coronograptus gregarius* Biozone of Bornholm (Denmark). Given that *P. sequens* is the only species that allows recognition of the *triangulatus* Biozone (i.e. the base of the Aeronian) at the current GSSP and that it may be occurring at a somewhat different stratigraphical level at Hlásná Třebaň than in Wales, this casts further doubt on the reliability of the current GSSP as a reliable marker for international correlation.

Rastrites longispinus (the stratigraphically lowest species of *Rastrites* in Europe), *D. brevis* and *C. rostratus* have their lowest occurrences 20 cm above the base of the Aeronian succession in the Hlásná Třebaň section, which is within the lower third of the *triangulatus* Biozone. *Rastrites longispinus* is widespread in the *triangulatus* and *pectinatus* biozones of the broader European realm (peri-Gondwana, Avalonia and Baltica) and has also been reported in several palaeotropical regions, including Siberia (Obut *et al.* 1968; Sennikov 1976), Yukon, Canada (Lenz 1982) and South China (Liu *et al.* 2017). *Campograptus rostratus* has also been reported outside of Europe, in Siberia (Obut *et al.* 1967) and South China (Chen & Lin 1978), whereas *D. brevis* has not been previously recorded outside the lower and middle *triangulatus* Biozone of Great Britain (see Zalasiewicz *et al.* 2009).

The present results, together with evaluation of published data, have shown that correlation of the Hlásná Třebaň section will be possible at very high resolution, based on graptolite occurrence data, with other sections in the Prague Synform and those distributed from Morocco, Portugal and Spain through Italy, Serbia, Bulgaria and Turkey in the south across central Europe to east Baltic countries, Sweden, Denmark and Great Britain in the north. Correlation of the European graptolite sequence with those of North America, Siberia and China will require further systematic revisions of the faunas of those regions, but the apparent common occurrence of several species that closely bracket the boundary interval, including *P. concinnus*, *C. rostratus*, *R. longispinus*, and *P. ovatoelongatus*, as well as the earliest forms of *Demirastrites*, suggests that very high-resolution correlation should be possible among these regions as well.

Correlatable Rhuddanian–Aeronian boundary strata worldwide

Anoxic black shales rich in planktonic graptolites are particularly widespread in the lowermost Silurian (Melchin *et al.* 2013), and the same litho- and biofacies continue through the Rhuddanian–Aeronian boundary interval in many parts of the world. Surprisingly though, few Rhuddanian–Aeronian boundary sections have been studied in sufficient detail to be correlated precisely with the succession exposed at Hlásná Třebaň and adjacent sections in the Prague Synform. Some of the sections referred to below are those relevant to prospective high-resolution and quantitative correlation (Melchin *et al.* 2016) based on published data, and others show the potential for precise correlation but require more detailed sampling and systematic work.

Great Britain

A continuous sequence of Rhuddanian–Aeronian boundary strata crops out in Rheidol Gorge, east of Aberystwyth in mid Wales. The succession alternates between grey bioturbated mudstones and black shales with a common and highly diverse graptolite fauna representing the *C. cyphus* and *D. triangulatus* biozones, as well as overlying strata. Although the rocks are cleaved and low-grade metamorphosed, both graptolites and associated chitinozoans of *Spinachitina maennili* Biozone are moderately to well-preserved (Melchin *et al.* 2016). Sudbury (1958) published a list of graptolite taxa recorded from her *gregarius* Biozone, which roughly corresponds with the *triangulatus*, *magnus* and *leptotheca* biozones of Zalasiewicz *et al.* (2009) and Loydell (2012). Sudbury marked the base of the *gregarius* Biozone by the FAD of '*Monograptus separatus separatus*' followed at a somewhat higher level, by the FAD of '*Monograptus separatus triangulatus*'. Both forms were considered by Melchin *et al.* (2016) to represent variants of *D. triangulatus* and that taxonomic opinion is followed here. Sudbury (1958) also reported the occurrence of several other taxa in the lower-middle part of what would be recognized here as the *triangulatus* Biozone, including *P. concinnus*, *C. gregarius*, *P. sudburiae* (=*M. revolutus* C), and *Dem*? *brevis*. Both *P. ovatoelongatus* and *R. longispinus* were reported from the middle part of the *gregarius* Biozone in association with *D. pectinatus* (= *fimbriatus*), *C. communis* and *R. longispinus*. The Rheidol Gorge section is currently being studied as another candidate for the base Aeronian GSSP (Melchin *et al.* 2016).

Toghill (1968) described the lower and middle Llandovery succession of the Birkhill Shales at Dob's Linn near Moffat, southern Scotland. He recognized the upper Rhuddanian *cyphus* Biozone, which is closely comparable with the *cyphus* Biozone as recognized in this paper. Black mudstones of the *cyphus* Biozone are separated by ca. 0.3-m-thick claystone with calcareous nodules, which is lacking in graptolites, from the overlying black mudstones of the *gregarius* Biozone. The base of the *gregarius* Biozone is marked by the lowest occurrence of *D. triangulatus* s.l., whereas *C. gregarius* is reported first occurring in the middle *cyphus* Biozone. The *gregarius* Zone of Toghill, however, includes higher levels with *D. pectinatus* (senior name to *M. fimbriatus*), and *N. magnus* in its upper part. In addition to the biostratigraphical data, the Dob's Linn section has been demonstrated to show a weak, but significant positive excursion in $\delta^{13}C_{org}$ values of similar magnitude as those recorded here, which occurs at a level near the FAD of *D. triangulatus* s.l. (Heath 1998; Melchin & Holmden 2006).

Central, Western and Southern Europe, Northwestern Peri-Gondwana

A rather condensed and tectonized succession of hemipelagic black clayey and siliceous shales and cherts with abundant graptolites occurs in Thuringia and Vogtland, Germany. Rhuddanian–Aeronian boundary beds have been described from several sections near Ronneburg and Hohenleuben by Schauer (1971). The graptolite fauna appears to be closely related to that of the Bohemian sections, but detailed comparison suffers from effects of tectonic strain on Thuringian graptolites. The uppermost Rhuddanian strata belong in the *cyphus* Biozone. The early Aeronian *gregarius* Biozone is marked by common occurrence of *D. triangulatus* associated with *D. pectinatus*. However, some reported graptolite occurrences, such as that of *Petalolithus minor* in the middle part of the *cyphus* Biozone, and *C. cyphus*, *H. acinaces* and *P. difformis* from the lower *triangulatus* Biozone, call for further fieldwork and taxonomic study of the fauna.

Graptolite-bearing black-shale sections through the Rhuddanian–Aeronian boundary strata have also been recorded in the Carnic Alps (Oberbuchach section of Jaeger & Schönlaub 1980) and in the Seville Province of Spain (sections around El Pintado reservoir in Valle Syncline, Jaeger & Robardet 1979). Both sections are in need of more detailed work to be correlated with proper resolution.

North Africa and Saudi Arabia – Northwestern Gondwana

Moderately condensed black siliceous shales and silicites, including Rhuddanian–Aeronian boundary beds are developed in central Morocco. Willefert (1963) described age-diagnostic graptolite taxa including *P. inopinatus*, *P. obuti* (named therein as *P. mutabilis*), *P. ovatoelongatus*, *C. cyphus*, *P.* cf. *revolutus*, *D. triangulatus*, *D. pectinatus* (named therein as *D. fimbriatus*), *D. major*, *C. rostratus* and *R. longispinus* (named therein as *R. approximatus*), accompanied by *R. toernquisti* and *C. gregarius*, from the Kasba-Tadla-Azrou anticlinorium. A similar fauna was discovered at the Jbel Ousserdoune section exposed in the Tazekka Inlier (P. Štorch personal observation, 2016). However, no section has been studied with relevant resolution. Muddy marine shelf deposits of late Rhuddanian and early Aeronian age, which extend from Libya, through Tunisia, Algeria and southern Morocco to Mauritania, yield low-to-moderate diversity assemblages dominated by biserial graptolites (Willefert 1963; Legrand 1999; Štorch & Massa 2003) with limited correlative potential.

Williams *et al.* (2016) analysed graptolite data from 66 boreholes in Saudi Arabia. The authors recognized a rather condensed *cyphus* Biozone (≤0.3 m in thickness) and up to 2-metres-thickness of *triangulatus* Biozone strata in the Rhuddanian–Aeronian boundary interval. The *cyphus* Biozone was defined by the total range of the name-giving species, which is accompanied by *N. fezzanensis*, *D. confertus* s.l., *R. toernquisti, A. atavus*, *P. revolutus*, *P. sudburiae*, and the earliest occurrences of *C. gregarius.* The *triangulatus* Biozone is marked by the lowest occurrence of *D. triangulatus*, followed by *R. longispinus* and several other taxa, including *Paraclimacograptus libycus* (Desio 1940) – an important clue for correlation with low-diversity fauna of North Africa. The overlying strata have been assigned to the *Neodiplograptus thuringiacus* Biozone (Williams *et al.* 2016), which corresponds, at least in part, with our *pectinatus* Biozone, as suggested by the co-occurrence of *D. pectinatus* (named therein as *D. fimbriatus*) with *D. triangulatus*, *R. longispinus* and *P. ovatoelongatus.*

Northeastern Europe, sections located on Baltica

Rhuddanian–Aeronian boundary strata, intermittently exposed on Bornholm, were described in a comprehensive graptolite paper by Bjerreskov (1975). The poorly exposed upper Rhuddanian succession has been assigned to *P. revolutus* Biozone as *C. cyphus* is very rare on Bornholm and in Sweden. The lowermost Aeronian was referred to the *gregarius* Biozone, the base of which is indicated by almost simultaneous lowest occurrences of *C. gregarius* and *D. triangulatus* s.s. As a result, Bjerreskov (1975) divided her *gregarius* Biozone into a lower *triangulatus* Subzone and an upper *pectinatus* Subzone, both of which correspond well with the biozones as recognized in Bohemia. The FAD of *P. ovatoelongatus* closely follows that of *D. triangulatus*, whereas *R. longispinus* appears higher, in the upper part of the *triangulatus* Subzone.

The subsurface extent of upper Rhuddanian and Aeronian mudrocks with graptolites and chitinozoans has been documented in numerous drill cores in Latvia and Lithuania. Moderate diversity graptolite faunas of the *cyphus* and *triangulatus* biozones, described by Paškevičius (1979), exhibit close similarity to those of the peri-Gondwanan Europe, although some taxonomic reassessment is needed. The middle and upper parts of the *triangulatus* Biozone, in the sense of Paškevičius (1979), correspond with *pectinatus*, *simulans* and perhaps also the *leptotheca* biozones of Štorch (2006) and this paper. This conclusion is based on the occurrence of several marker species of the *leptotheca* Biozone, including *Campograptus millepeda* and *Petalolithus folium* (Hisinger 1837), which were reported from the upper *triangulatus* Biozone. The suggested base of the Aeronian Stage and the whole *triangulatus* Biozone correlate with a level within *Aspelundia expansa* conodont Biozone, and possibly near the boundary between the *Euconochitina electa* and *Ancyrogchitina convexa* chitinozoan biozones as shown by integrated graptolite, conodont and chitinozoan data from the Aizpute-41 core of Latvia published by Loydell *et al.* (2003). In addition to the biostratigraphical data, a core from a predominantly carbonate succession in Estonia also records a weak positive $\delta^{13}C_{carb}$ excursion near the base of the Aeronian (Kaljo & Martma 2000), which Melchin & Holmden (2006) suggested may be correlative with that observed in the $\delta^{13}C_{org}$ records in Arctic Canada, also evident in the Hlásná Třebaň section.

China, Yangtze Platform

A large number of richly fossiliferous sections across the Rhuddanian–Aeronian boundary interval are available in the Chinese Yangtze Platform. Detailed knowledge of these sections is lacking as most of the focus of earlier authors has been the late Katian and Hirnantian succession and the Ordovician–Silurian boundary interval. The Rh–Ae boundary strata occur within a rather uniform, offshore, black-shale succession of the lower and middle Llandovery Lungmachi Formation throughout the Yangtze Platform region (Fan *et al.* 2011).

Chen & Lin (1978) defined the '*Pristiograptus*' *cyphus* – '*Monoclimacis*' *lunata* Biozone in the upper Rhuddanian of Tongzi area of northern Guizhou Province. The rich graptolite assemblage of that biozone, however, included genera typical of Aeronian strata elsewhere in the world (*Petalolithus*, *Rastrites* and triangulate monograptids of *D. triangulatus* affinity). Hence, the base of the Aeronian Stage likely occurs within the *cyphus–lunata* Biozone of Chen & Lin (1978). The *C. gregarius* Biozone recognized in the lower Aeronian succession was divided into the lower *Rastrites guizhouensis* and upper *D. triangulatus* subzones. The graptolite assemblages differ markedly from those of Baltica, Avalonia and peri-Gondwanan Europe in both the species represented and in relative diversity and abundance of the genera.

Ni (1978) studied the graptolites of Lungmachi Formation from the Yichang (Yangtze Gorges) area of the western Hubei Province. The location of the Rh–Ae boundary remained unclear as *Rastrites* (*R. cirratus* Ni 1978) was reported from an interval assigned to the upper Rhuddanian *Pristiograptus leei* Zone, whereas monograptids of the *D. triangulatus* group were missing in the lower Aeronian *triangulatus* Biozone of Ni (1978). Wang (1985) reported the *D. triangulatus* Biozone from Yangtze Gorges and reconciled the Rhuddanian and Aeronian graptolite biozonation of the area with the international standard (see Loydell 2012), although notable differences in graptolite faunas did not allow for high-resolution correlation with European sections.

The Rhuddanian and Aeronian black shales of the Lungmachi Formation exposed in Guanyinqiao, in Qijiang District of Sichuan Province, were documented by Jin *et al.* (1982). Both the sediments and graptolite fauna are consistent with those encountered in other regions of south-central China. The *cyphus* and *leei* biozones have been recognized in the upper Rhuddanian and the lower Aeronian commenced with the *triangulatus* Biozone, overlain by the *C. communis* Biozone. The base of the Aeronian is marked by FAD of *D. triangulatus*, followed by abundant rastritids. *Petalolithus palmeus qijiangensis* Zhao, 1982 (in Jin *et al.* 1982), reported from the uppermost Rhuddanian *leei* Biozone, closely resembles robust rhabdosomes of *P. obuti* or *P. mutabilis*.

In connection with the current search for a new Aeronian GSSP, well-exposed hemipelagic black shales of the Rh–Ae boundary interval, rich in well-preserved graptolites and chitinozoans, are being studied in detail in the Shennongjia Section in northwestern Hubei, and also the Shuanghe and Yuxiancun sections in southeastern Sichuan. Recently published data from a drill core in southeastern Sichuan showed a weak, but significant positive excursion in $\delta^{13}C_{org}$ values of similar magnitude as those recorded here at a level that is also near the FAD of *D. triangulatus* (Liu *et al.* 2016), thus extending the correlation potential of the carbon isotope record in this interval more globally.

Siberia

Silty shales rich in upper Rhuddanian and lower Aeronian graptolites were documented by Sennikov (1976) from several sections in Gorny Altai, although the Rh–Ae boundary interval has never been studied in particular detail in this region. The *triangulatus* Biozone, overlying the upper Rhuddanian *cyphus* Biozone, is marked by the FADs of triangulate monograptids, petalolithids and rastritids. However, specimens assigned by Sennikov (1976) to *D. pectinatus* are confined in the lower part of the *triangulatus* Biozone in contrast to European records of the species, which come for the most part from above the range of *D. triangulatus*. Subsequent revision of the biostratigraphy of the region, based upon the richly fossiliferous reference section near Ust-Chagirka (Obut & Sennikov 1985), introduced a combined *triangulatus-gregarius* Biozone embracing all Aeronian strata up to the base of the *L. convolutus*–*C. cometa* Biozone.

Numerous drill cores from the Norilsk area (southwestern Siberian Platform) extending through Rh–Ae boundary strata were documented by Obut *et al.* (1968). The lower Silurian succession, which rests unconformably on middle Ordovician shales and/or limestones, begins with dark grey calcareous shales of the upper Rhuddanian *cyphus* Biozone and/or lower Aeronian *triangulatus* Biozone. The Rh–Ae boundary was recorded in nine boreholes. Rich and well-preserved graptolite faunas were described by Obut *et al.* (1968), which exhibit some similarity in species composition and relative abundance to faunal assemblages of the Yangtze Platform, although no attempt has been made for rigorous systematic comparison. No actual specimens of *C. cyphus* were recorded in the *cyphus* Assemblage Zone. The base of the Aeronian is marked by the almost simultaneous lowest occurrences of *Demirastrites* (specimens assigned to *D. triangulatus* and *D. pectinatus* by the latter authors), *C. gregarius* and *P. ovatoelongatus*, closely followed by *R. longispinus* and '*Stavrites*' *rossicus* Obut and Sobolevskaya, 1968 (in Obut *et al.* 1968). *Campograptus* first appears in a stratigraphically higher part of the *triangulatus* Biozone.

Northern Canada

Rhuddanian–Aeronian successions of dark grey to black calcareous shales with thin limestone interbeds exposed on Cornwallis Island, Nunavut were documented by Melchin (1989). New data pertaining specifically to the Rh–Ae boundary interval were presented by Melchin & MacRae (2014). Boundary strata are marked by a sequence of closely spaced FADs of *P. concinnus*, *D. triangulatus* and *Petalolithus* sp. The base of the *triangulatus* Biozone coincides closely with a weak positive shift in $\delta^{13}C_{org}$ values reported by Melchin & Holmden (2006), which is similar in magnitude to the one reported here at Hlásná Třebaň.

Black shales of the Rhuddanian–Aeronian boundary interval exposed in the northern Canadian Cordillera of the Yukon and Northwest Territories were documented by Lenz (1979). The uppermost Rhuddanian was assigned to the *gregarius* Biozone, which is overlain by the lowermost Aeronian *triangulatus* Biozone. Detailed descriptions of the sections are not available to date. The graptolite fauna described by Lenz (1982) exhibits notable similarities to apparently coeval assemblages of China (Yangtze Platform), Siberia and the Canadian Arctic Islands.

Conclusions

We propose that the Hlásná Třebaň section should be considered as a GSSP for the base of the Aeronian – the second stage of the Silurian System. The suggested base of the Aeronian Stage is selected 1.38 m above the base of the black-shale succession of the Želkovice Formation, at the level in the section corresponding with the lowest occurrence of *Demirastrites triangulatus*, which defines the base of the *D. triangulatus* graptolite Biozone. Data from Bohemia, together with an overview of published records worldwide, have shown that *D. triangulatus* is a widely applicable and potentially easily recognizable tool for stratigraphical correlation and that its FAD at the proposed GSSP is closely bracketed by the first and last occurrences of several other taxa, some of which are widely geographically distributed. The FAD of *D. triangulatus* occurs just below a minor positive shift in $\delta^{13}C_{org}$ values recorded in the lower part of the *triangulatus* Biozone, which also appears to be recognizable in several different parts of the world. The lower *triangulatus* Biozone clearly exhibits a rapid graptolite diversification event with the closely spaced appearances of several new lineages: monograptids with isolated and hooked thecae (genera *Demirastrites, Rastrites* and *Campograptus*) as well as species of *Petalolithus*.

Combined redox element proxies [Ce/Ce*, V (V+Ni), V/Cr, Th/U] suggest that the Rhuddanian black shales and silty-micaceous laminites of the Hlásná Třebaň section were deposited under anoxic to euxinic bottom conditions. High TOC values (ca. 6 wt.%), recorded in the middle and upper Rhuddanian strata (upper *vesiculosus* and *cyphus* biozones) may be indicative of high palaeoproductivity despite apparently condensed sedimentation. A subsequent stepwise decrease of TOC to about 4 wt. % started from the lowermost Aeronian lower *triangulatus* Biozone. In the same interval a minor but significant $\delta^{13}C$ positive excursion is recorded, along with slightly weakened anoxia suggested by gradual shift in redox-sensitive element ratios. The lithology of the lower Aeronian black shales changed gradually towards more siliceous lithotypes, including alternation of siliceous shale and silty silicite in the uppermost *pectinatus* and *simulans* biozones. The changing lithology is also reflected in the rock magnetic susceptibility record, which results from an increasing proportion of diamagnetic quartz cement. The lithology, detrital input and redox element proxies indicate gradual and relatively minor environmental and depositional changes in the late Rhuddanian and early Aeronian. In addition, the $\delta^{15}N_{bulk}$ record supports the interpretation that the succession was deposited under primarily anoxic bottom-water conditions and also that there was no significant change in the community of primary producers throughout the studied time interval. Other Bohemian sections that span the Rhuddanian–Aeronian boundary interval (Karlík, Vočkov near Karlštejn, Zadní Třebaň, Černošice and Nové Butovice) archive sedimentary and graptolite records that are fully consistent with that described from the proposed stratotype.

The graptolite succession of Hlásná Třebaň, and other sections of the Prague Synform, can be readily correlated to sections in the Welsh Basin, where the current GSSP occurs, although the current GSSP itself contains a poor and ambiguous biostratigraphical record through the boundary interval. The graptolite record across the boundary is more complete in Bohemia, enabling high-resolution and nearly worldwide correlation based on both biostratigraphical and, potentially, chemostratigraphical data.

Acknowledgements. – We greatly appreciate the financial support provided by the Czech Science Foundation through project 14-16124S. PŠ and LC appreciate subsequent in-house support received from the Institute of Geology of the Czech Academy of Sciences (RVO 67985831). ŠM, ZT and JF appreciate in-house support received from the Czech Geological Survey (SRP Project no. 339900). MJM acknowledges the financial support of a Natural Sciences and Engineering Research Council (Canada) Discovery Grant. We are indebted to V. Turek and L. Váchová (National Museum, Prague) who photographed shale slab in Figure 6. Mr. J. Kotek (Prague) kindly assisted in the field. Brad Cramer and an unnamed reviewer are thanked for their helpful comments on the earlier version of the manuscript.

References

Aïfa, T., Pruner, P., Chadima, M. & Štorch, P. 2007: Structural evolution of the Prague Synform (Czech Republic) during Silurian times: an AMS, rock magnetism, and palaeomagnetic study of the Svatý Jan pod Skalou dikes. *In* Linnemann, U., Nance, R.D., Kraft, P. & Zulauf, G. (eds): *The Evolution of the Rheic Ocean: from Avalonian–Cadomian Active Margin to Alleghenian–Variscan Collision. Special Papers Geological Society of America, 423*, 249–265.

Algeo, T.J. & Maynard, J.B. 2004: Trace-element behavior and redox facies in core shales of Upper Pennsylvanian Kansas-type cyclothems. *Chemical Geology 206*, 289–318.

Bau, M. & Dulski, P. 1996: Distribution of yttrium and rare-earth elements in the Penge and Kuruman iron-formations, Transvaal Supergroup, South Africa. *Precambrian Research 79*, 37–55.

Bhatia, M.R. & Crook, K.A.W. 1986: Trace element characteristics of graywackes and tectonic setting discrimination of sedimentary basins. *Contributions to Mineralogy and Petrology 92*, 181–193.

Bjerreskov, M. 1975: Llandoverian and Wenlockian graptolites from Bornholm. *Fossils and Strata 8*, 1–94.

Bouček, B. 1944: Über einige gedornte Diplograptiden des böhmischen und sächsischen Silurs. *Mitteilungen der Tschechischen Akademie der Wissenschaften für 1943 53*, 1–6.

Bouček, B. 1953: Biostratigraphy, development and correlation of the Želkovice and Motol Beds of the Silurian of Bohemia. *Sborník Ústředního Ústavu Geologického, Oddíl Paleontologický 20*, 421–484.

Bouček, B. & Přibyl, A. 1942: O Petalolithech ze skupiny *P. folium* (His.) a o rodu *Cephalograptus* Hopk. *Rozpravy České Akademie věd a umění, Třída 2, für 1942, 51*, 1–23.

Brenchley, P.J. & Štorch, P. 1989: Environmental changes in the Hirnantian (upper Ordovician) of the Prague Basin, Czechoslovakia. *Geological Journal 24*, 165–181.

Butcher, A. 2016: Chitinozoan data from the Hlásná Třebaň section, Czech Republic – a potential replacement GSSP for the base of the Aeronian stage (Llandovery Series, Silurian). *In* Guerdebeke, P., De Weirdt, J., Vandenbroucke, T.R.A. & Cramer, B.D. (eds): *IGCP 591 The Early to Middle Paleozoic Revolution, Closing Meeting*, Ghent University, Belgium, 6–9 July 2016, Abstracts, 29. Ghent University, Ghent.

Calvert, S.E. & Pedersen, T.F. 1993: Geochemistry of Recent oxic and anoxic marine sediments: implications for the geological record. *Marine Geology 113*, 67–88.

Calvert, S.E. & Pedersen, T.F. 2007: Elemental proxies for palaeoclimatic and palaeoceanographic variability in marine sediments: interpretation and application. *Developments in Marine Geology 1*, 597–644.

Capone, D., Bronk, D., Mulholland, M. & Carpenter, E. (eds) 2008: *Nitrogen in the Marine Environment*, 2nd edn, 1757 pp. Elsevier, Amsterdam.

Chen, X. & Lin, Y.K. 1978: Lower Silurian graptolites from Tongzi, northern Guizhou. *Memoir of the Nanjing Institute of Geology and Palaeontology, Academia Sinica 12*, 1–106 [in Chinese with English Abstract].

Chlupáč, I., Havlíček, V., Kříž, J., Kukal, Z. & Štorch, P. 1998: *Palaeozoic of the Barrandian (Cambrian to Devonian)*, 183 pp. Czech Geological Survey, Prague.

Cocks, L.R.M. & Torsvik, T.H. 2002: Earth geography from 500 to 400 million years ago: a faunal and paleomagnetic review. *Journal of Geological Society 159*, 631–644.

Cocks, L.R.M. & Torsvik, T.H. 2006: European geography in a global context from the Vendian to the end of Palaeozoic. *In* Gee, D.G. & Stephenson, R.A. (eds): *European Lithosphere Dynamics. Geological Society Memoirs 32*, 83–95.

Cocks, L.R.M., Woodcock, N.H., Rickards, R.B., Temple, J.T. & Lane, P.D. 1984: The Llandovery Series of the type area. *Bulletin of the British Museum (Natural History), Geology Series 38*, 131–182.

Cooper, R.A., Sadler, P.M., Munnecke, A. & Crampton, J.S. 2014: Graptolite evolutionary rates track Ordovician-Silurian global climate change. *Geological Magazine 151*, 349–364.

Cowie, J.A., Ziegler, W., Boucot, A.J., Bassett, M.G. & Remane, J. 1986: Guidelines and statuses of the International Commission on Stratigraphy (ICS). *Courier Forschungsinstitut Senckenberg 83*, 1–14.

Cramer, B.D., Brett, C.E., Melchin, M.J., Männik, P., Kleffner, M.A., McLaughlin, P.I., Loydell, D.K., Munnecke, A., Jeppsson, L., Corradini, C., Brunton, F.R. & Saltzman, M.R. 2011: Revised correlation of Silurian Provincial Series of North America with global and regional chronostratigraphic units and δ^{13} Ccarb chemostratigraphy. *Lethaia 44*, 185–202.

Davies, K.A. 1929: Notes on the graptolite faunas of the Upper Ordovician and Lower Silurian. *Geological Magazine 66*, 1–27.

Davies, J.R., Waters, R.A., Zalasiewicz, J.A., Molyneux, S.G., Vandenbroucke, T.R.A. & Williams, M. 2011a: A revised sedimentary and biostratigraphical architecture for the type Llandovery and Garth areas, central Wales: a field guide. *British Geological Survey Open Report*, OR/10/037.

Davies, J.R., Ray, D.C., Thomas, A.T., Loydell, D.K., Cherns, L., Cramer, B.D., Veevers, S.J., Worton, G.J., Marshall, C., Molyneux, S.G., Vandenbroucke, T.R.A., Verniers, J., Waters, R.A., Williams, M. & Zalasiewicz, J.A. 2011b: *Siluria Revisited: A Field Guide*, 170 pp. International Subcommission on Silurian Stratigraphy, London.

Davies, J.R., Waters, R.A., Molyneux, S.G., Williams, M., Zalasiewicz, J.A., Vandenbroucke, T.R.A. & Verniers, J. 2013: A revised sedimentary and biostratigraphical architecture for the Type Llandovery area, Central Wales. *Geological Magazine 150*, 300–332.

Desio, A. 1940: Fossili neosilurici del Fezzan occidentale. *Annali del Museo Libico di Storia Naturale 2*, 13–45.

Drost, K. 2008: Sources and geotectonic setting of Late Neoproterozoic-Early Paleozoic volcano-sedimentary successions of the Teplá-Barrandian Unit (Bohemian Massif): evidence from petrographical, geochemical, and isotope analyses. *Geologica Saxonica 54*, 1–165.

Dufka, P. & Fatka, O. 1993: Chitinozoans and acritarchs from the Ordovician-Silurian Boundary of the Prague Basin, Czech Republic. *Special Papers in Palaeontology 48*, 17–28.

Dufka, P., Kříž, J. & Štorch, P. 1995: Silurian graptolites and chitinozoans from the Uranium Industry boreholes drilled in 1968–1971 (Prague Basin, Bohemia). *Bulletin of the Czech Geological Survey 70*, 5–13.

Ebbestad, J.O.R., Frýda, J., Wagner, P.J., Horný, R.J., Isakar, M., Stewart, S., Percival, I.G., Bertero, V., Rohr, D.M., Peel, J.S., Blodgett, R.B. & Högström, A.E.S. 2013: Biogeography of Ordovician and Silurian gastropods, monoplacophorans and mimospirids. *In* Harper, D.A.T. & Servais, T. (eds): *Early Palaeozoic biogeography and palaeogeography. Geological Society Memoirs 38*, 199–220.

Eisel, R. 1912: Über zonenweise Entwicklung der Rastriten und Demirastriten. *Jahresberichte der Gesellschaft von Freunde der Naturwissenschaften in Gera 53/54*, 27–43.

Elles, G.L. 1897: The subgenera *Petalograptus* and *Cephalograptus*. *Quarterly Journal of the Geological Society of London 53*, 186–212.

Elles, G.L. & Wood, E.M.R. 1906: A monograph of British graptolites. *Monograph of the Palaeontographical Society*. Part 5, *60*, 181–216, pls 26–27.

Elles, G.L. & Wood, E.M.R. 1907: A monograph of British graptolites. *Monograph of the Palaeontographical Society*. Part 6, *61*, 217–272, pls 28–31.

Elles, G.L. & Wood, E.M.R. 1913: A monograph of British graptolites. *Monograph of the Palaeontographical Society*. Part 9, *66*, 415–486, pls 42–49.

Eriksson, M.E., Hints, O., Paxton, H. & Tonarová, P. 2013: Ordovician and Silurian polychaete diversity and biogeography. *In* Harper, D.A.T. & Servais, T. (eds): *Early Palaeozoic biogeography and palaeogeography. Geological Society Memoirs 38*, 265–272.

Fan, J.X., Melchin, M.J., Chen, X., Wang, Y., Zhang, Y.D., Chen, Q., Chi, Z.L. & Chen, F. 2011: Biostratigraphy and geography of the Ordovician-Silurian Lungmachi black shales in South China. *Science China; Earth Sciences 54*, 1854–1863.

Fatka, O. & Mergl, M. 2009: The, microcontinent' Perunica: status and story 15 years after conception. *In* Bassett, M.G. (ed.): *Early Palaeozoic Peri-Gondwana Terranes: New Insights from tectonics and Biogeography*. *Geological Society, London, Special Publications 325*, 65–101.

Floyd, P.A. & Leveridge, B.E. 1987: Tectonic environment of the Devonian Gramscatho basin, south Cornwall: framework mode and geochemical evidence from turbiditic sandstones. *Journal of the Geological Society 144*, 531–542.

Frýda, J. & Štorch, P. 2014: Carbon isotope chemostratigraphy of the Llandovery in northern peri-Gondwana: new data from the Barrandian area, Czech Republic. *Estonian Journal of Earth Sciences 63*, 220–226.

Goldman, D., Maletz, J., Melchin, M.J. & Fan, J.X. 2013: Graptolite palaeobiogeography. *In* Harper, D.A.T. & Servais, T. (eds): *Early Palaeozoic biogeography and palaeogeography*. *Geological Society Memoirs 38*, 415–428.

Gutierrez-Marco, J.C. & Štorch, P. 1998: Graptolite biostratigraphy of the Lower Silurian (Llandovery) shelf deposits of the Western Iberian Cordillera, Spain. *Geological Magazine 135*, 71–92.

Harkness, R. 1851: Description of the graptolites found in the black shales of Dumfriesshire. *Quarterly Journal of the Geological Society of London 7*, 58–65.

Havlíček, V., Vaněk, J. & Fatka, O. 1994: Perunica microcontinent in the Ordovician (its position within the Mediterranean Province, series division, benthic and pelagic associations). *Sborník Geologických věd, Geologie 46*, 23–56.

Heath, R.J. 1998: *Palaeoceanographic and Faunal Changes in the Early Silurian*. Unpublished Ph.D. Thesis, University of Liverpool, Liverpool.

Hisinger, H. 1837: *Lethaea Suecica seu Petrifacta Suecica, Supplementum* 1. Stockholm, 124 pp.

Holland, C.H. & Bassett, M.G. 1989: A global standard for the Silurian system. *National Museum of Wales Geological Series 10*, 1–325.

Hopkinson, J. 1869: On British graptolites. *Journal of Quekett Microscopic Club 1*, 151–166.

Horný, R. 1956: Zóna *Akidograptus ascensus* v jižním křídle barrandienského siluru. *Věstník Ústředního Ústavu Geologického 31*, 62–69.

Hutt, J.E. 1974: A new group of Llandovery biform monograptids. *In* Rickards, R.B., Jackson, D.E. & Hughes, C.P. (eds): *Graptolite Studies in honour of O.M.B. Bulman*. *Special Papers in Palaeontology 13*, 189–203.

Hutt, J.E. 1975: The Llandovery graptolites of the English Lake District, Part 2. *Monograph of the Palaeontographical Society 129*, 57–137.

Jaeger, H. & Robardet, M. 1979: Le Silurien et le Dévonien basal dans le Nord de la Province de Séville (Espagne). *Géobios 12*, 687–714.

Jaeger, H. & Schönlaub, H.P. 1980: Silur und Devon nördlich der Gundersheimer Alm in den Karnischen Alpen (Österreich). *Carinthia II 170/90*, 404–444.

Janoušek, V., Farrow, M.C. & Erban, V. 2006: Interpretation of whole-rock geochemical data in igneous geochemistry: introducing Geochemical Data Toolkit (GCDkit). *Journal of Petrology 47*, 1255–1259.

Jin, C.T., Ye, S.H., He, Y.X., Wan, Z.Q., Wang, S.B., Zhao, Y.T., Li, S.J., Xu, X.Q. & Zhang, Z.G. 1982: *The Silurian Stratigraphy and Paleontology in Guanyinqiao, Qijiang, Sichuan*, 84. People's Publishing House of Sichuan, Chengdu.

Jones, O.T. 1909: The Hartfell-Valentian succession in the district around Plynlimon and Pont Erwyd (North Cardiganshire). *Quarterly Journal of the Geological Society of London 65*, 463–537.

Jones, B. & Manning, D.A.C. 1994: Comparison of geochemical indices used for the interpretation of palaeoredox conditions in ancient mudstones. *Chemical Geology 111*, 111–129.

Kaljo, D. & Martma, T. 2000: Carbon isotopic composition of Llandovery rocks (East Baltic Silurian) with environmental interpretation. *Proceedings of the Estonian Academy of Sciences, Geology 49*, 267–283.

Kendall, M.G. 1975: *Rank Correlation Methods*, 160 pp. Griffin, London.

Kirste, E. 1919: Die Graptolithen des Altenburger Ostkreises. *Mitteilungen aus der Osterlande, N.F. 16*, 60–222.

Kodym, O., Bouček, B. & Šulc, J. 1931: Guide to the geological excursion to the neighbourhood of Beroun, Koněprusy and Budňany. *Knihovna Státního Geologického Ústavu Československé Republiky 15*, 1–83.

Koren', T.N. & Bjerreskov, M. 1997: Early Llandovery monograptids from Bornholm and the southern Urals: taxonomy and evolution. *Bulletin of the Geological Society of Denmark 44*, 1–43.

Koren', T.N. & Rickards, R.B. 1996: Taxonomy and evolution of Llandovery biserial graptoloids from the southern Urals, western Kazakhstan. *Special Papers in Palaeontology 54*, 1–103.

Kříž, J. 1975: Revision of the Lower Silurian stratigraphy in central Bohemia. *Věstník Ústředního Ústavu Geologického 50*, 275–283.

Kříž, J. 1992: Silurian field excursions: Prague Basin (Barrandian), Bohemia. *National Museum Wales, Geological Series 13*, 1–111.

Kříž, J. 1998: Silurian. *In* Chlupáč, I., Havlíček, V., Kříž, J., Kukal, Z. & Štorch, P. (eds): *Palaeozoic of the Barrandian (Cambrian to Devonian)*, 79–101. Czech Geological Survey, Prague.

Kröger, B. 2013: Cambrian–Ordovician cephalopod palaeogeography and diversity. *In* Harper, D.A.T. & Servais, T. (eds): Early Palaeozoic biogeography and palaeogeography. *Geological Society Memoirs 38*, 429–448.

Krs, M. & Pruner, P. 1995: Palaeomagnetism and palaeogeography of the Variscan formations of the Bohemian Massif, comparison with other European regions. *Journal of Geosciences 40*, 3–46.

Krs, M. & Pruner, P. 1999: To the paleomagnetic investigations of paleogeography of the Barrandian Terrane, Bohemian Massif. *Acta Universitatis Carolinae, Geologica 43*, 519–522.

Krs, M., Pruner, P. & Man, O. 2001: Tectonic and palaeogeographic interpretation of the paleomagnetism of Variscan and pre-Variscan formations of the Bohemian Massif, with special reference to the Barrandian Terrane. *Tectonophysics 332*, 93–114.

Kurck, C. 1882: Några nya graptolitarter från Skåne. *Geologiska Föreningens i Stockholm Förhandlingar 6*, 294–304.

Lapworth, C. 1876: On Scottish Monograptidae. *Geological Magazine 3*, 308–321, 350–360, 499–507, 544–552.

Lapworth, H. 1900: The Silurian sequence of Rhayader. *Quarterly Journal of the Geological Society of London 56*, 67–137.

Legrand, P. 1977: Contribution à l'etude des graptolites du Llandoverien inferieur de l'Oued In Djerane (Tassili N'ajjer oriental, Sahara algérien). *Bulletin de la Société D'Histoire Naturelle de L'Afrique du Nord 67*, 141–196.

Legrand, P. 1999: *Approche stratigraphique de l'Ordovicien terminal et du Silurien inferieur du Sahara algérien par l'étude des Diplograptides (Graptolites)*. DSc Thesis. d'Etat. Université Michel de Montaigne, Bordeaux 3, Inst. EGID, 892 pp.

Lenz, A.C. 1979: Llandoverian graptolite zonation in the northern Canadian Cordillera. *Acta Palaeontologica Polonica 24*, 137–153.

Lenz, A.C. 1982: Llandoverian graptolites of the Northern Canadian cordillera: *Petalograptus*, *Cephalograptus*, *Rhaphidograptus*, *Dimorphograptus*, Retiolitidae, and Monograptidae. *Life Sciences Contributions, Royal Ontario Museum 130*, 1–154.

Linnemann, U., Romer, R.L., Gehmlich, M. & Drost, K. 2004: Paläogeographie und Provenance des Saxothuringikums unter besonderer Beachtung der Geochronologie von prävariszischen Zirkonen und der Nd-Isotopie von Sedimenten. *In* Linnemann, U. (ed.): *Das Saxothuringikum: Abriss der präkambrischen und paläozoischen Geologie von Sachsen and Thüringen*. *Geologica Saxonica 48/49*, 121–132.

Liu, Y., Li, C., Algeo, T.J., Fan, J.X. & Peng, P.A. 2016: Global and regional controls on marine redox changes across the Ordovician-Silurian boundary in South China. *Palaeogeography Palaeoclimatology Palaeoecology 463*, 180–191.

Liu, Z.H., Algeo, T.J., Guo, X.S., Fan, J.X., Du, X.B. & Lu, Y.C. 2017: Paleo-environmental cyclicity in the Early Silurian Yangtze Sea (South China): tectonic or glacio-eustatic control? *Palaeogeography, Palaeoclimatology, Palaeoecology 466*, 59–76.

Loader, C.R. 1999: *Local Regression and Likelihood*, 290 pp. Springer, Berlin.

Loydell, D.K. 2012: Graptolite biozone correlation charts. *Geological Magazine 149*, 124–132.

Loydell, D.K., Männik, P. & Nestor, V. 2003: Integrated biostratigraphy of the lower Silurian of the Aizpute-41 core, Latvia. *Geological Magazine 140*, 205–229.

Luo, G.M., Algeo, T.J., Zhan, R.B., Yan, D., Huang, J.H., Liu, J.S. & Xie, S.C. 2016: Perturbation of the marine nitrogen cycle during the Late Ordovician glaciation and mass extinction. *Palaeogeography, Palaeoclimatology, Palaeoecology 448*, 339–348.

MacRae, N.D., Nesbitt, H.W. & Kronberg, B.I. 1992: Development of a positive Eu anomaly during diagenesis. *Earth and Planetary Science Letters 109*, 585–591.

Manck, E. 1923: Untersilurische Graptolithenarten der Zone 10 des Obersilurs, ferner *Diversograptus* gen. nov. sowie einige neue Arten anderer Gattungen. *Natur (Leipzig) 14*, 282–289.

Mann, H.B. 1945: Nonparametric tests against trend. *Econometrica 13*, 245–259.

M'Coy, F. 1850: On some new genera and species of Silurian Radiata in the collection of the University of Cambridge. *Annals and Magazine of Natural History 6*, 270–290.

Meidla, T., Tinn, O., Salas, M.J., Williams, M., Siveter, D., Vandenbroucke, T.R.A. & Sabbe, K. 2013: Biogeographical patterns of Ordovician ostracods. *In* Harper, D.A.T. & Servais, T. (eds): *Early Palaeozoic Biogeography and Palaeogeography*. *Geological Society Memoirs 38*, 337–354.

Melchin, M.J. 1989: Llandovery graptolite biostratigraphy and palaeobiogeography, Cape Phillips Formation, Canadian Arctic Islands. *Canadian Journal of Earth Science 26*, 1726–1746.

Melchin, M.J. & Holmden, C. 2006: Carbon isotope chemostratigraphy of the Llandovery in Arctic Canada: implications for global correlation and sea-level change. *GFF 128*, 173–180.

Melchin, M.J. & MacRae, K.D. 2014: Insights into the Rhuddanian-Aeronian and Aeronian-Telychian boundary intervals from eastern and Arctic Canada. *In* Zhan, R.B. & Huang, B. (eds): *IGCP 591 Field Workshop 2014, Kunming China, Extended Summary*, 86–88. Nanjing University Press, Nanjing.

Melchin, M.J., Sadler, P.M. & Cramer, B.D. 2012: The Silurian period. *In* Gradstein, F.M., Ogg, J.G. & Smith, A.G. (eds): *A Geologic Time Scale 2012*, 525–558. Elsevier, Amsterdam.

Melchin, M., Mitchell, C.E., Holmden, C. & Štorch, P. 2013: Environmental changes in the Late Ordovician – early Silurian: review and new insights from black shales and nitrogen isotopes. *The Geological Society of America Bulletin 125*, 1635–1670.

Melchin, M.J., Boom, A., Davies, J.R., De Weirdt, J., McIntyre, A.J., Morgan, G., Phillips, S., Russell, C., Vandenbroucke, T.R.A., Williams, M. & Zalasiewicz, J.A. 2016: Integrated stratigraphic study of the Rhuddanian-Aeronian (Llandovery, Silurian) boundary succession at Rheidol Gorge, Wales. *In* Guerdebeke, P., De Weirdt, J., Vandenbroucke, T.R.A. & Cramer, B.D. (eds): *IGCP 591 The Early to Middle Paleozoic Revolution, Closing Meeting*, Ghent University, Belgium, 6–9 July 2016, Abstracts, 60–61. Ghent University, Ghent.

Molyneux, S.G., Delabroye, A., Wicander, R. & Servais, T. 2013: Biogeography of early to mid Palaeozoic (Cambrian–Devonian) marine phytoplankton. *In* Harper, D.A.T. & Servais, T. (eds): *Early Palaeozoic Biogeography and Palaeogeography*. *Geological Society Memoirs 38*, 365–397.

Murphy, J.B., Gutiérrez-Alonso, G., Nance, R.D., Fernandez-Suarez, J., Keppie, J.D., Quesada, C., Strachan, R.A. & Dostal, J. 2006: Origin of the Rheic Ocean: rifting along a Neoproterozoic suture? *Geology 34*, 325–328.

Ni, Y.N. 1978: Lower Silurian graptolites from Yichang, western Hubei. *Acta Palaeontologica Sinica 17*, 387–420 [in Chinese with English Abstract].

Nicholson, H.A. 1867: On some fossil from the Lower Silurian rocks of the South of Scotland. *Geological Magazine 1*, 107–113.

Nicholson, H.A. 1868a: On the graptolites of the Coniston Flags; with notes on the British species of the genus *Graptolites*. *Quarterly Journal of the Geological Society of London 24*, 521–545.

Nicholson, H.A. 1868b: On the nature and zoological position of the Graptolitidae. *Annals and Magazine of Natural History 4*, 55–61.

Nicholson, H.A. 1869: On some new species of graptolites. *Annals and Magazine of Natural History 4*, 231–242.

Obut, A.M. 1965: Graptolity silura Omulevskikh gor (Bassein reky Kolymy). *In*: *Stratigrafia i Paleontologia Asiatskoy chasti USSR*. Izd. Nauka, 33–46. Moskva.

Obut, A.M. & Sennikov, N.V. 1985: Graptolite zones in the Ordovician and Silurian of the Gorny Altai. *In* Hughes, C.P. & Rickards, R.B. (eds): Palaeoecology and Biostratigraphy of Graptolites. *Geological Society Special Publication 20*, 155–164.

Obut, A.M., Sobolevskaya, R.F. & Nikolaev, A.A. 1967: *Graptolity i Stratigrafiya Nizhnego Silura Okrainnykh Podnyatii Kolymskogo Massiva*, 164 pp. Akademiya Nauk SSR, Sibirskoje Otdelenie, Institut Geologii i Geofiziki, Ministerstvo Geologii SSSR, Nauchno-Issledovatel'sky Institut Geologii Arktiki, Moskva.

Obut, A.M., Sobolevskaya, R.F. & Merkureva, A.P. 1968: *Graptolity Llandoveri v Kernakh Burovykh Skvazhin Norilskogo Rayona*, 162 pp. Akademia nauk USSR, Sibirskoe ottdelenie, Institut geologii i geofyziki, Moskva.

Oczlon, M. 1992: Examples of Palaeozoic contourites, tempestites and turbidites – classification and palaeogeographic approach. *Heidelberger Geowissenschaftliche Abhandlungen 53*, 57–159.

Paškevičius, J. 1979: *Biostratigraphy and Graptolites of the Lithuanian Silurian*, 267 pp. Mosklas, Vilnius [in Russian].

Patočka, F., Pruner, P. & Štorch, P. 2003: Palaeomagnetism and geochemistry of Early Palaeozoic rocks of the Barrandian (Teplá–Barrandian Unit, Bohemian Massif): palaeotectonic implications. *Physics and Chemistry of the Earth 28*, 735–749.

Pedersen, T.B.P. 1922: Rastritesskiferen pa Bornholm. *Meddelelser fra Dansk Geologisk Forening 6*, *11*, 3–29.

Perner, J. 1897: *Études sur les graptolites de Boheme. Part* 3, *Section* A. Prag, 25 pp.

Přibyl, A. 1937: O stratigrafických poměrech vrstev želkovických eα1 u Hlásné Třebaně. *Věstník Státního Geologického Ústavu 13*, 4.

Přibyl, A. 1941: O českých a cizích zástupcích rodu *Rastrites* Barrande, 1850. *Rozpravy České Akademie věd a Umění, Třída 251*, 1–21.

Přibyl, A. 1942: *Pernerograptus* nov. gen. a jeho zástupci z českého a cizího siluru. *Věstník Královské České společnosti nauk. Třída matematicko-přírodovědecká* 1941, 1–18.

Přibyl, A. & Münch, A. 1941: Revize středoevropských zástupců rodu *Demirastrites* Eisel. *Rozpravy České Akademie věd a Umění, Třída 2 51*, 1–29.

von Raumer, J. & Stampfli, G.M. 2008: The birth of the Rheic Ocean – early Palaeozoic subsidence patterns and subsequent tectonic plate scenarios. *Tectonophysics 461*, 9–20.

Richter, R. 1853: Thüringische Graptolithen. *Zeitschrift der Deutschen Geologischen Gesellschaft 5*, 439–464.

Rickards, R.B. & Koren', T.N. 1974: Virgellar meshworks and sicular spinosity in Llandovery graptoloids. *Geological Magazine 111*, 193–204.

Rickards, R.B., Hutt, J.E. & Berry, W.B.N. 1977: Evolution of the Silurian and Devonian graptoloids. *Bulletin of the British Museum (Natural History), Geology 28*, 1–120.

Robardet, M. 2003: The Armorica microplate: fact or fiction? Critical review of the concept and contradictory palaeobiogeographical data. *Palaeogeography, Palaeoclimatology, Palaeoecology 195*, 25–148.

Rong, J.Y., Melchin, M.J., Williams, S.H., Koren', T.N. & Verniers, J. 2008: Report of the restudy of the defined global stratotype of the base of the Silurian System. *Episodes 31*, 315–318.

Russel-Houston, J. 2001: *Taphonomy and Evolution of Some Early Silurian Graptolites from Cornwallis Island, Arctic Canada*. Unpublished Ph.D. Thesis, Dalhousie University, Halifax.

Salvador, A. (ed.) 1994: *International Stratigraphic Guide*, 2nd edn, 214. IUGS and Geological Society of America, Boulder.

Schauer, M. 1971: Biostratigraphie und Taxionomie der Graptolithen des tieferen Silurs unter besonderer Berucksichtigung der tektonischen Deformation. *Freiberger Forschungshefte, C273 Paläontologie*, 1–185.

Sennikov, N.V. 1976: *Graptolites and Lower Silurian Stratigraphy of the Gorny Altai*, 274 pp. Nauka Press, Moskva [in Russian].

Sennikov, N.V., Yolkin, E.A., Petrunina, Z.E., Gladkikh, L.A., Obut, O.T., Izokh, N.G. & Kipriyanova, T.P. 2008: *Ordovician-Silurian Biostratigraphy and Paleogeography of the Gorny Altai*, 156 pp. Publishing House SB RAS, Novosibirsk.

Stampfli, G.M., von Raumer, J. & Borel, G.D. 2002: Paleozoic evolution of pre-Variscan terranes: from Gondwana to the Variscan collision. *In* Martínez Catalán, J.R., Hatcher, R.D. Jr., Arenas, R. & Díaz García, F. (eds): Variscan–Appalachian Dynamics: The Building of the Late Paleozoic Basement. *Special Papers Geological Society of America 364*, 263–280.

Štorch, P. 1983: The genus *Diplograptus* (Graptolithina) from the lower Silurian of Bohemia. *Věstník Ústředního Ústavu Geologického 58*, 159–170.

Štorch, P. 1985: *Orthograptus* s.l. and *Cystograptus* (Graptolithina) from the Bohemian lower Silurian. *Věstník Ústředního Ústavu Geologického 60*, 87–99.

Štorch, P. 1986: Ordovician-Silurian boundary in the Prague Basin (Barrandian area, Bohemia). *Sborník Geologických Věd, Geologie 41*, 69–103.

Štorch, P. 1988: Earliest Monograptidae (Graptolithina) in the lower Llandovery sequence of the Prague Basin. *Sborník Geologických Věd, Paleontologie 29*, 9–48.

Štorch, P. 1991: *Faciální vývoj, stratigrafie a korelace svrchního ordoviku a spodního siluru pražské pánve (Barrandien)*. Unpublished PhD Thesis, Czech Geological Survey, Prague, 232 pp.

Štorch, P. 1994: Graptolite biostratigraphy of the Lower Silurian (Llandovery and Wenlock) of Bohemia. *Geological Journal 29*, 137–165.

Štorch, P. 1996: The basal Silurian *Akidograptus ascensus – Parakidograptus acuminatus* Biozone in peri-Gondwanan Europe: graptolite assemblages, stratigraphical ranges and palaeobiogeography. *Bulletin of the Czech Geological Survey 71*, 171–178.

Štorch, P. 1998: Graptolites of the *Pribylograptus leptotheca* and *Lituigraptus convolutus* biozones of Tmaň (Silurian, Czech Republic). *Journal of the Czech Geological Society 43*, 209–272.

Štorch, P. 2006: Facies development, depositional settings and sequence stratigraphy across the Ordovician-Silurian boundary: a new perspective from Barrandian area of the Czech Republic. *Geological Journal 41*, 163–192.

Štorch, P. 2015: Graptolites from Rhuddanian-Aeronian boundary interval (Silurian) in the Prague Synform, Czech Republic. *Bulletin of Geosciences 90*, 841–891.

Štorch, P. & Frýda, J. 2012: The late Aeronian graptolite sedgwickii Event, associated positive carbon isotope excursion and facies changes in the Prague Synform (Barrandian area, Bohemia). *Geological Magazine 149*, 1089–1106.

Štorch, P. & Kraft, P. 2009: Graptolite assemblages and Stratigraphy of the lower Silurian Mrákotín Formation, Hlinsko Zone, NE interior of the Bohemian Massif (Czech Republic). *Bulletin of Geosciences 84*, 51–74.

Štorch, P. & Massa, D. 2003: Biostratigraphy, Correlation, Environmental and Biogeographic Interpretation of the Lower Silurian Graptolite Faunas of Libya. *In* Salem, M.J. & Oun, K.M. (eds): The Geology of Northwest Libya, Vol. *1*, 237–251.

Štorch, P. & Serpagli, E. 1993: Lower Silurian graptolites from Southwestern Sardinia. *Bolletino Della Società Paleontologica Italiana 32*, 3–57.

Suchý, V., Sýkorová, I., Stejskal, M., Šafanda, J., Machovič, V. & Novotný, M. 2002: Dispersed organic matter from Silurian shales of the Barrandian basin, Czech Republic: optical properties, chemical composition and thermal maturity. *International Journal of Coal Geology 53*, 1–25.

Sudbury, M. 1958: Triangulate monograptids from the *Monograptus gregarius* Zone (Lower Llandovery) of the Rheidol Gorge (northern Cardiganshire). *Philosophical Transactions of the Royal Society of London, Series B 241*, 485–555.

Sverjensky, D.A. 1984: Europium redox equilibria in aqueous solution. *Earth and Planetary Science Letters 67*, 70–78.

Tait, J., Bachtadse, V. & Soffel, H.C. 1994: Silurian palaeogeography of Armorica – new palaeomagnetic data from Central Bohemia. *Journal of Geophysical Research: Solid Earth 99*, 2897–2907.

Tait, J., Bachtadse, V. & Soffel, H.C. 1995: Upper Ordovician palaeogeography of the Bohemian Massif – implications for Armorica. *Geophysical Journal International 122*, 211–218.

Tasáryová, Z., Schnabl, P., Čížková, K., Pruner, P., Janoušek, V., Rapprich, V., Štorch, P., Manda, Š., Frýda, J. & Trubač, J. 2014: Gorstian palaeoposition and geotectonic setting of Suchomasty Volcanic Centre (Silurian, Prague Basin, Teplá-Barrandian Unit, Bohemian Massif). *GFF 136*, 262–265.

Taylor, S.R. & McLennan, S.M. 1985: *The Continental Crust: Its Composition and Evolution*, 1–312. Blackwell, Oxford.

Temple, J.T. 1988: Biostratigraphical correlation and stages of the Llandovery. *Journal of the Geological Society of London 145*, 875–879.

Toghill, P. 1968: The graptolite assemblages and zones of the Birkhill Shales (Lower Silurian) at Dobb's Linn. *Palaeontology 11*, 654–668.

Törnquist, S.L. 1897: On the diplograptidae and heteroprionidae of the scanian rastrites beds. *Lunds Universitets Årsskrifter 33*, 1–24.

Törnquist, S.L. 1899: Researches into the monograptidae of the scanian rastrites beds. *Lunds Universitets Arsskrifter 35*, 1–25.

Törnquist, S.L. 1907: Observations on the genus *Rastrites* and some allied species of *Monograptus*. *Lunds Universitets Årsskrifter (NS), Afd. 2, 3, 5*, 1–22.

Torsvik, T.H. & Cocks, L.R.M. 2013: New global palaeogeographical reconstructions for the Early Palaeozoic and their generation. *In* Harper, D.A.T. & Servais, T. (eds): Early Palaeozoic Biogeography and Palaeogeography. *Geological Society, London, Memoirs 38*, 5–24.

Wang, X.F. 1985: Lower Silurian graptolite zonation in the eastern Yangzi (Yangtze) Gorges, China. *Bulletin of the Geological Society of Denmark 35*, 231–243.

Wignall, P.B. 1994: *Black Shales*, 127 pp. Oxford University Press, Oxford.

Wignall, P.B. & Twitchett, R.J. 1996: Oceanic anoxia and the end of Permian mass extinction. *Science 272*, 1155–1158.

Wignall, P.B., Newton, R. & Brookfield, M.E. 2005: Pyrite framboid evidence for oxygen-poor deposition during the Permian-Triassic crisis in Kashmir. *Palaeogeography, Palaoeclimatology, Palaeoecology 216*, 183–188.

Wilkin, R.T., Barnes, H.L. & Brantley, S.L. 1996: The size distribution of framboidal pyrite in modern sediments: an indicator of redox conditions. *Geochimica et Cosmochimica Acta 60*, 3897–3912.

Willefert, S. 1963: Les Graptolites du Silurien inférieur duj bel Eguer-Iguiguena (SW d'Ito, anticlinorium de Kasba-Tadla-Azrou, Maroc central). *Notes et Memoires du Service Géologique 177*, 1–74.

Williams, M., Zalasiewicz, J., Boukhamsin, H. & Cesari, C. 2016: Early Silurian (Llandovery) graptolite assemblages of Saudi Arabia: biozonation, palaeoenvironmental significance and biogeography. *Geological Quarterly 60*, 3–25.

Zalasiewicz, J. 1992: Two new graptolites from the early Silurian (Llandovery: Aeronian) of central Wales: an origin for monoclimacid thecal morphology. *Geological Magazine 129*, 779–785.

Zalasiewicz, J. 1996: Aeronian (Silurian, Llandovery) graptolites from central Wales. *Geologica et Palaeontologica 30*, 1–14.

Zalasiewicz, J.A. & Tunnicliff, S. 1994: Uppermost Ordovician to Lower Silurian graptolite biostratigraphy of the Wye Valley, central Wales. *Palaeontology 37*, 695–720.

Zalasiewicz, J.A., Taylor, L., Rushton, W.A., Loydell, D.K., Rickards, R.B. & Williams, M. 2009: Graptolites in British stratigraphy. *Geological Magazine 146*, 785–850.

Supporting Information

Additional Supporting Information may be found in the online version of this article:

Table S1. Whole-rock major- and trace-element analyses (ppm, respectively) for the Hlásná Třebaň shale samples.

Table S2. $\delta^{13}C_{org}$, $\delta^{15}N_{bulk}$, TOC and N analytical data from the Hlásná Třebaň section.